






Bounded-degree plane geometric spanners in practice*

Frederick Anderson , Anirban Ghosh , Matthew Graham ,
Lucas Mougeot , and David Wisnosky 

School of Computing
University of North Florida
Jacksonville, FL, USA

✉ {n01451351, anirban.ghosh, n00612546, n01398041, n01153911}@unf.edu

Abstract

The construction of bounded-degree plane geometric spanners has been a focus of interest since 2002 when Bose, Gudmundsson, and Smid proposed the first algorithm to construct such spanners. To date, eleven algorithms have been designed with various trade-offs in degree and stretch factor. We have implemented these sophisticated algorithms in C++ using the CGAL library and experimented with them using large synthetic and real-world pointsets. Our experiments have revealed their practical behavior and real-world efficacy. We share the implementations via [GitHub](#)¹ for broader uses and future research.

We present a simple practical algorithm, named APPXSTRETCHFACTOR, that can estimate stretch factors (obtains lower bounds on the exact stretch factors) of geometric spanners – a challenging problem for which no practical algorithm is known yet. In our experiments with bounded-degree plane geometric spanners, we find that APPXSTRETCHFACTOR estimates stretch factors almost precisely. Further, it gives linear runtime performance in practice for the pointset distributions considered in this work, making it much faster than the naive Dijkstra-based algorithm for calculating stretch factors.

Keywords — geometric graph, plane spanner, stretch factor, experimental algorithmics

1 Introduction

Let G be the complete Euclidean graph on a given set P of n points embedded in the Euclidean plane. A *geometric t -spanner* on P is a geometric graph $G' := (P, E)$, a subgraph of G such that for every pair of points $u, v \in P$, the distance between them in G' (the Euclidean length of a shortest path between u, v in G') is at most t times their Euclidean distance $|uv|$, for some $t \geq 1$. It is easy to check that G itself is a 1-spanner with $\Theta(n^2)$ edges. The quantity t is referred to as the *stretch factor* of G' . If there is no need to specify t , we simply use the term *geometric spanner* and assume that there exists some t for G' . We say that G' is *plane* if it is crossing-free. G' is *degree- k* or is said to have *bounded-degree* if its degree is at most k . In this work, we experiment with bounded-degree plane geometric spanners. See Figure 1 for an example of such a spanner.

Bounded-degree plane geometric spanners have been an area of interest in computational geometry for a long time. Non-crossing edges make them suitable for wireless network applications where edge crossings create communication interference. The absence of crossing edges also makes them useful for the design of road networks to eliminate high-budget flyovers. Such spanners have $O(n)$ edges (at most $3n - 6$ edges); as a result, they are less expensive to store and navigate. Further, shortest-path algorithms run quicker on them since they are sparse. Bounded-degree helps in reducing on-site equipment costs.

Bose, Gudmundsson, and Smid [13] were the first to show that there always exists a plane geometric $\sigma(\pi + 1)$ -spanner of degree at most 27 on any pointset, where σ denotes an upper bound for the stretch factor

*Research supported by the University of North Florida Academic Technology Grant and NSF Award CCF-1947887. Visualizations of some of the implemented algorithms were demonstrated at the 37th International Symposium on Computational Geometry (SoCG 2021) in Media Exposition.

¹<https://github.com/ghoshanirban/BoundedDegreePlaneSpannersCppCode>

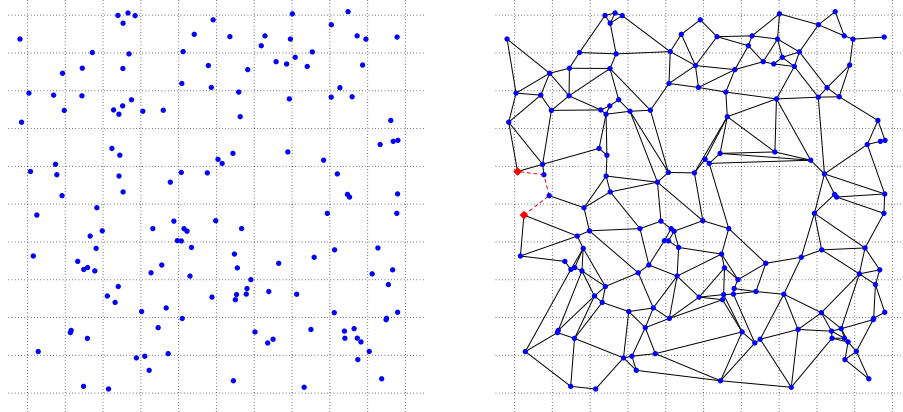


Figure 1: Left: A set P of 150 points, generated randomly within a square. Right: A plane degree-6 spanner on P with stretch factor ≈ 1.82 . The pair of points for which the spanner achieves a stretch factor of ≈ 1.82 is shown in red along with the shortest path between them.

of L_2 -Delaunay triangulations² (the current best known value is $\sigma = 1.998$ due to Xia [44]). This result was subsequently improved in a long series of papers [9, 12, 14, 16, 33, 34, 36] in terms of degree and/or stretch factor. Bonichon et al. [11] reduced the degree to 4 with $t \approx 156.8$. Soon after this, Kanj et al. improved this stretch factor upper bound to 20 in [32]. A summary of these results is presented in Table 1. This family of spanner construction algorithms has turned out to be a fascinating application of the Delaunay triangulation. Note that all these algorithms produce bounded-degree plane subgraphs of the complete Euclidean graph on P with constant stretch factors.

| REFERENCE | DEGREE | STRETCH FACTOR |
|---|--------|---|
| Bose, Gudmundsson, and Smid [13] | 27 | $\sigma(\pi + 1) \approx 8.3$ |
| Li and Wang [36] | 23 | $\sigma(1 + \frac{\pi}{\sqrt{2}}) \approx 6.4$ |
| Bose, Smid, and Xu [16] | 17 | $\sigma(2 + 2\sqrt{3} + \frac{3\pi}{2} + 2\pi \sin \frac{\pi}{12}) \approx 23.6$ |
| Kanj, Perković, and Xia [33] | 14 | $\sigma(1 + \frac{2\pi}{14 \cos(\pi/14)}) \approx 2.9$ |
| Kanj and Xia [34] | 11 | $\sigma(\frac{2 \sin(2\pi/5) \cos(\pi/5)}{2 \sin(2\pi/5) \cos(\pi/5) - 1}) \approx 5.7$ |
| Bose, Hill, and Smid [14] | 8 | $\sigma(1 + \frac{2\pi}{6 \cos(\pi/6)}) \approx 4.4$ |
| Bose, Carmi, and Chaitman-Yerushalmi [12] | 7 | $\sigma(1 + \sqrt{2})^2 \approx 11.6$ |
| Bose, Carmi, and Chaitman-Yerushalmi [12] | 6 | $\sigma(\frac{1}{1 - \tan(\pi/7)(1 + 1/\cos(\pi/14))}) \approx 81.7$ |
| Bonichon, Gavoille, Hanusse, and Perković [9] | 6 | 6 |
| Bonichon, Kanj, Perković, and Xia [11] | 4 | $\sqrt{4 + 2\sqrt{2}(19 + 29\sqrt{2})} \approx 156.8$ |
| Kanj, Perković, and Türkoğlu [32] | 4 | 20 |

Table 1: A summary of results on constructions of bounded-degree plane geometric spanners, sorted by the degree they guarantee. The best known upper bound of $\sigma = 1.998$ for the stretch factor of the L_2 -Delaunay triangulation [44] is used in this table for expressing the stretch factors.

The intriguing question that remains to be answered is whether the degree can be reduced to 3 while keeping t bounded; refer to [15, Problem 14] and [42, Chapter 32]. Interestingly, if one does not insist on constructing a *plane* spanner, Das and Heffernan [23] showed that degree 3 is always achievable. Narasimhan and Smid [39, Section 20.1] show that no degree-2 plane spanner of the infinite integer lattice can have a constant stretch factor. Thus, a minimum degree of 3 is necessary to achieve a constant stretch factor. If P is convex, then it is always possible to construct a degree-3 plane geometric spanners, see [4, 7, 32].

²A triangulation T for a pointset P is referred to as a L_2 -Delaunay triangulation if no point in P lies inside the circumcircle of any triangle in T .

From the other direction, lower bounds on the stretch factors of plane spanners for finite pointsets have been investigated in [24, 25, 35, 37]. In-browser visualizations of some of the algorithms (those based on the L_2 -Delaunay triangulation) have been recently presented in [3]. In related works, the construction of plane hop spanners (where the number of hops in shortest paths is of interest) for unit disk graphs has been considered in [6, 19, 26].

The most notable experimental work for geometric spanners is done by Farshi and Gudmundsson [27]. The authors engineered and experimented with some of the well-known geometric spanners construction algorithms published before 2009. However, the authors did not use the algorithms considered in this work in their experiments. Planarity and bounded-degree are important concerns in geometric network design. Hence, we found it motivating to implement the eleven algorithms (refer to Table 1) meant to construct bounded-degree plane geometric spanners. Asymptotic runtimes and various theoretical bounds do not always do justice in explaining the real-world performance of algorithms, especially in computational geometry, because of heavy floating-point operations needed for various geometric calculations. Experiments reveal their real-world performance. A unique aspect of the family of bounded-degree plane spanner construction algorithms is that users cannot specify an arbitrary value of t and/or degree for spanner construction. It is a deviation from many standard spanner algorithms; see [12, 39] for a review of such algorithms. This makes experiments with them even more interesting.

Our contributions. (i) We experimentally compare the aforementioned eleven bounded-degree plane spanner construction algorithms by implementing them carefully in C++ using the popular CGAL library [41] and running them on large synthetic and real-world pointsets. The largest pointset contains 1.9 million points approximately. For broader uses of these sophisticated algorithms, we share the C++ implementations via GitHub³. The comparisons are performed based on their runtimes and degree, stretch factor, and lightness of the generated spanners. We present a brief overview of the algorithms implemented and our experimental results in Sections 2 and 4, respectively.

(ii) In doing experiments with spanners, we find that stretch factor measurement turns out to be a severe bottleneck when n is large. To address this, we have designed a new fast algorithm named APPXSTRETCH-FACTOR that can estimate the stretch factor of a given spanner (not necessarily plane). In our experiments, we find that it can estimate stretch factors with high accuracy for the class of geometric spanners dealt with in this work. It is considerably faster than the naive Dijkstra-based exact stretch factor measurement algorithm in practice. To our knowledge, no such practical algorithm exists in the literature. Further, it can be easily parallelized, making it very useful for estimating stretch factors of large spanners. See Section 3 for a description of this algorithm.

2 Algorithms implemented

Every algorithm designed to date for constructing bounded-degree plane geometric spanners relies on some variant of Delaunay triangulation. The rationale behind this is that such triangulations are geometric spanners [10, 21, 22, 44] and are plane by definition. As a result, the family of plane spanner construction algorithms considered in this work has turned out to be a fascinating application of Delaunay triangulation. It is essential to know that Delaunay triangulations have unbounded degrees and cannot be used as bounded-degree plane spanners.

In this section, we provide a brief description for each of the eleven algorithms considered in this work. Appropriate abbreviations using the authors' names and dates of publication are used for naming purposes. Since most of these algorithms are involved, so we urge the reader to refer to the original papers for a deeper understanding and correctness proofs. For visualizing some of these algorithms, we recommend the interactive in-browser applet⁴ developed by us; refer to [3]. To observe variations in spanner construction between the algorithms see Appendix 6.1.

In these algorithms, the surrounding of every input point is frequently divided into multiple cones (depending on the algorithm) for carefully selecting edges from the Delaunay triangulation used as the starting

³<https://github.com/ghoshanirban/BoundedDegreePlaneSpannersCppCode>

⁴<https://ghoshanirban.github.io/bounded-degree-plane-spanners/index.html>

point. In our pseudocodes, the cone i of point u , considered clockwise, is denoted by C_i^u . A triangulation T of a pointset P is said to be a L_2 -Delaunay triangulation of P if no point in P lies inside the circumcircle of any triangle in T . Eight of the eleven algorithms use L_2 -Delaunay triangulation as the starting point. The remaining three use L_∞ or TD -Delaunay triangulations, as described later in this section. In the following, n denotes the size of the input pointset.

- **BGS05: Bose, Gudmundsson, and Smid** [13]. This was the first algorithm that can construct bounded-degree plane spanners using the classic L_2 -Delaunay triangulation. First, a Delaunay triangulation DT of P is constructed. Next, a degree-3 spanning subgraph SG of DT is computed that contains the convex hull of P and is a (possibly degenerate) simple polygon with P as its vertex set. The polygon is then transformed into a simple non-degenerate polygon Q . The vertices of Q are processed in an order that is obtained from a breadth-first order of DT , and then Delaunay edges are carefully added to Q . The resulting graph denoted G' , is a plane spanner for the vertices of Q . Refer to Algorithm 5 for a pseudocode of this algorithm. The authors show that their algorithm generates degree-27 plane spanners with a stretch factor of $1.998(\pi + 1) \approx 8.3$ and runs in $O(n \log n)$ time.

Algorithm 1: CanonicalOrdering(DT)

```

1 Allocate  $\Phi[1, \dots, n]$ ;
2 Make a copy of  $DT$  and call it  $H$ ;
3 Let reserved be a set of two consecutive vertices  $v_1, v_2$  on the convex hull of  $H$ ;
4  $\Phi_1 \leftarrow v_1, \Phi_2 \leftarrow v_2$ ;
5 for  $i = 1$  to  $n - 2$  do
6   | Let  $u$  be a vertex of the outer face of  $H \setminus$  reserved that is adjacent to at most two other vertices on the
7   |   outer face;
8   |    $\Phi_u \leftarrow n - i + 1$ ;
9   |   Remove  $u$  and all incident edges from  $H$ ;
10 end
11 return  $\Phi$ ;
```

Algorithm 2: SpanningGraph(DT)

```

1  $\Phi[1, \dots, n] \leftarrow$  CanonicalOrdering( $DT$ ) (Algorithm 1);
2  $SG \leftarrow \emptyset$ ;
3 Add edges between  $v_1, v_2, v_3 \in \Phi$  to  $SG$  and mark the vertices as done;
4 for  $v_i \in \Phi \setminus \{v_1, v_2, v_3\}$  do
5   | Let  $u_1, \dots, u_k$  be the vertices neighboring  $v_i$  in  $DT$  marked as done;
6   | Remove edge  $\{u_1, u_2\}$  from  $SG$ ;
7   | Add edges  $\{v_i, u_1\}$  and  $\{v_i, u_2\}$  to  $SG$ ;
8   | if  $k > 2$  then
9   |   | Remove edge  $\{u_{k-1}, u_k\}$  from  $SG$ ;
10  |   | Add edge  $\{v_i, u_k\}$  to  $SG$ ;
11  | end
12 end
13 return  $SG$ ;
```

- **LW04: Li and Wang** [36]. This algorithm is inspired from BSG2005 but is a lot simpler and avoids the use of intermediate (possibly degenerate) polygons. The algorithm computes a reverse low degree ordering of the vertices of the L_2 -Delaunay triangulation DT constructed on P . Then it sequentially considers the vertices in this ordering, divides the surrounding of every such vertex into multiple cones, and then adds short edges from DT to preserve planarity. Refer to Algorithm 7 for a pseudocode of this algorithm. The authors have shown that this algorithm generates degree-23 plane spanners (when the input parameter α of this algorithm is set to $\pi/2$) having a stretch factor of $1.998(1 + \pi/\sqrt{2}) \approx 6.4$ and runs in $O(n \log n)$ time.
- **BSX09: Bose, Smid, and Xu** [16]. This algorithm is quite similar to LW04 in design and also relies on reverse low-degree ordering of the vertices of the Delaunay triangulation. Refer to Algorithm 8. The authors have

Algorithm 3: TransformPolygon(SG, DT)

```
1  $V \leftarrow \emptyset, E \leftarrow \emptyset;$ 
2 Let  $s_1, v_1$  be two consecutive vertices on the convex hull of  $SG$  in counterclockwise order;
3  $v_{prev} \leftarrow s_1, v_i \leftarrow v_1;$ 
4 Add  $v_{prev}$  to  $V;$ 
5 do
6   Add  $v_i$  to  $V;$ 
7   Add  $\{v_i, v_{prev}\}$  to  $E;$ 
8   Let  $v_{next}$  be the neighbor of  $v_i \in SG$  such that  $v_{next}$  is the next neighbor clockwise from  $v_{prev};$ 
9    $v_{prev} \leftarrow v_i, v_i \leftarrow v_{next};$ 
10 while  $v_{prev} \neq s_1$  and  $v_i \neq v_1;$ 
11  $E = E \cup \{\{v_i, v_{prev}\}\} \cup DT \setminus SG;$ 
12 return  $(V, E);$ 
```

Algorithm 4: PolygonSpanner(Q, SG)

```
1 Let  $V, E$  be the vertices and edges of  $Q$ , respectively;
2 Let  $\rho[1, \dots, n]$  be the breadth-first ordering of  $V$  in  $Q$ , starting at any vertex in  $V;$ 
3  $E' \leftarrow SG;$ 
4 foreach  $u \in \rho$  do
5   Let  $s_1, s_2, \dots, s_m$  be the clockwise ordered neighbors of  $u$  in  $Q;$ 
6    $s_j, s_k \leftarrow s_m;$ 
7   if  $u \neq \rho_1$  then
8     | Set  $s_j$  and  $s_k$  to the first and last vertex in the ordered neighborhood of  $u$  where  $s_j, s_k \in E';$ 
9   end
10  Divide  $\angle s_1 u s_j$  and  $\angle s_k u s_m$  into a minimum number of cones with maximum angle  $\pi/2;$ 
11  In each cone, add the shortest edge in  $E$  incident upon  $u$  to  $E'$  and all edges  $\{s_\ell, s_{\ell+1}\}$  such that
    |  $1 \leq \ell < j$  or  $k \leq \ell < m;$ 
12 end
13 return  $E';$ 
```

Algorithm 5: BGS05(P)

```
1  $DT \leftarrow L_2\text{-DelaunayTriangulation}(P);$ 
2  $SG \leftarrow \text{SpanningGraph}(DT)$  (Algorithm 2);
3  $Q \leftarrow \text{TransformPolygon}(SG, DT)$  (Algorithm 3);
4  $G' \leftarrow \text{PolygonSpanner}(Q, SG)$  (Algorithm 4);
5 return  $G';$ 
```

Algorithm 6: ReverseLowDegreeOrdering(DT)

```
1 Allocate  $\Phi[1 \dots n];$ 
2 Make a copy of  $DT$  and call it  $H;$ 
3 for  $i = 1$  to  $n$  do
4   | Let  $u$  be a vertex in  $H$  with minimal degree;
5   |  $\Phi[u] \leftarrow n - i + 1;$ 
6   | Remove  $u$  and all incident edges from  $H;$ 
7 return  $\Phi;$ 
```

Algorithm 7: LW04(P , $0 < \alpha \leq \pi/2$)

```
1  $DT \leftarrow L_2\text{-DelaunayTriangulation}(P)$ ;  
2  $\Phi[1 \dots n] \leftarrow \text{ReverseLowDegreeOrdering}(DT)$  (Algorithm 6);  
3  $E \leftarrow \emptyset$ ;  
4 foreach  $u \in \Phi$  do  
5   Divide the area surrounding  $u$  into sectors delineated by  $u$ 's already processed neighbors in  $DT$ ;  
6   Divide each sector into a minimum number of cones  $C_u^0, C_u^1, \dots$  with angle at most  $\alpha$ ;  
7   foreach  $C_u^i$  do  
8     Let  $v_1, v_2, \dots, v_m$  be the clockwise-ordered Delaunay neighbors of  $u$  in  $C_u^i$ ;  
9     Add an edge between  $u$  and the closest of such neighbors to  $E$ ;  
10    Add all edges  $\{v_j, v_{j+1}\}$  such that  $1 \leq j < m$  to  $E$ ;  
11  Mark  $u$  as processed;  
12 return  $E$ ;
```

generalized their algorithm so that it can construct bounded-degree plane spanners from any triangulation of P , not necessarily just the L_2 -Delaunay triangulation (although the L_2 -Delaunay triangulation is of primary interest to us). When the L_2 -Delaunay triangulation is used and the parameter α is set to $2\pi/3$, the algorithm generates degree-17 plane spanners having a stretch factor of $\sigma(2 + 2\sqrt{3} + \frac{3\pi}{2} + 2\pi \sin \frac{\pi}{12}) \approx 23.6$ in $O(n \log n)$ time. After computing the triangulation and the reverse low-degree ordering, at every vertex u , $\delta = \lceil 2\pi/\alpha \rceil$ Yao cones are initialized such that the closest unprocessed triangulation neighbor falls on a cone boundary and occupies both cones as the *short* edge, which is added to the spanner. In the remaining cones, the closest unprocessed neighbor of u in each cone is added. In all cones, special edges between pairs of neighbors of u are added to the spanner if both the neighbors are unprocessed.

Algorithm 8: BSX09(P , $0 < \alpha \leq 2\pi/3$)

```
1  $DT \leftarrow L_2\text{-DelaunayTriangulation}(P)$ ;  
2  $\Phi[1 \dots n] \leftarrow \text{ReverseLowDegreeOrdering}(DT)$  (use Algorithm 6);  
3  $E \leftarrow \emptyset$ ;  
4 foreach  $u \in \Phi$  do  
5   if  $u$  has unprocessed Delaunay neighbors then  
6     Let  $v_{closest}$  be the closest unprocessed neighbor to  $u$ ;  
7     Add the edge  $\{u, v_{closest}\}$  to  $E$ ;  
8     Divide the area surrounding  $u$  into a minimum number of cones  $C_u^0, C_u^1, \dots$  with angle at most  $\alpha$ , such  
        that  $v_{closest}$  is on the boundary between the first and last cones;  
9     foreach  $C_u^i$  except the first and last do  
10    if  $u$  has unprocessed neighbors in  $C_u^i$  then  
11      Let  $w$  be the closest unprocessed neighbor to  $u$  in the cone;  
12      Add edge  $\{u, w\}$  to  $E$ ;  
13    end  
14    Let  $v_0, v_1, \dots, v_{m-1}$  be the clockwise-ordered neighbors of  $u$ ;  
15    Add all edges  $\{v_j, v_{(j+1) \bmod m}\}$  to  $E$  such that  $0 \leq j < m$  and  $v_j, v_{(j+1) \bmod m}$  are unprocessed;  
16  end  
17 end  
18  Mark  $u$  as processed;  
19 end  
20 return  $E$ ;
```

- **BGHP10: Bonichon, Gavoille, Hanusse, and Perković** [9]. It was the first algorithm that deviated from the use of L_2 -Delaunay triangulation; instead, it used TD -Delaunay triangulation to select spanner edges, introduced by Chew back in 1989 [22]. For such triangulations, empty equilateral triangles are

used for characterization instead of empty circles, as needed in the case of L_2 -Delaunay triangulations. TD -Delaunay triangulations are plane 2-spanners but may have an unbounded degree. BGHP10 first extracts a degree-9 subgraph from the TD -Delaunay triangulation that has a stretch factor of 6. Then using some local modifications, the degree is reduced from 9 to 6 but the stretch factor remains unchanged. Refer to Algorithm 9. It uses internally Algorithms 10 - 16. In this algorithm, each edge incident to a node is charged to some cone of that node. The algorithm runs in $O(n \log n)$ time, as shown by the authors.

- KPX10: **Kanj, Perković, and Xia** [33]. For every vertex u in the L_2 -Delaunay triangulation, its surrounding is divided into $k \geq 14$ cones. In every nonempty cone of u , the shortest Delaunay edge incident on u is selected. After this, a few additional Delaunay edges are also selected using some criteria based on cone sequences. See Algorithm 17 for a complete description of this algorithm with the technical details. When k is set to 14, degree-14 plane spanners are generated having a stretch factor of $1.998 \left(1 + \frac{2\pi}{14 \cos(\pi/14)}\right) \approx 2.9$. Note that out of the 11 algorithms we have implemented in this work, this algorithm gives the best theoretical guarantee on the stretch factor; see Table 1. KPX10 runs in $O(n \log n)$ time.

Algorithm 9: BGHP10(P)

```

1  $DT \leftarrow TD\text{-DelaunayTriangulation}(P)$ ;
2  $E \leftarrow \emptyset$ ;
3 foreach nonempty cone  $i$  of vertex  $u \in DT$  where  $i \in \{1, 3, 5\}$  do
4   Add edge  $\{u, \text{closest}(u, i)\}$  to  $E$ ;
5    $\text{charge}(u, i) \leftarrow \text{charge}(u, i) + 1$ ;
6    $\text{charge}(\text{closest}(u, i), i + 3) \leftarrow \text{charge}(\text{closest}(u, i), i + 3) + 1$ ;
7   if  $\text{first}(u, i) \neq \text{closest}(u, i) \wedge \text{i-relevant}(\text{first}(u, i), u, i - 1)$  then
8     Add edge  $u, \text{first}(u, i)$  to  $E$ ;
9      $\text{charge}(u, i - 1) \leftarrow \text{charge}(u, i - 1) + 1$ ;
10  end
11 if  $\text{last}(u, i) \neq \text{closest}(u, i) \wedge \text{i-relevant}(\text{last}(u, i), u, i + 1)$  then
12   Add edge  $\{u, \text{last}(u, i)\}$  to  $E$ ;
13    $\text{charge}(u, i + 1) \leftarrow \text{charge}(u, i + 1) + 1$ ;
14 end
15 end
16 foreach cone  $i$  of vertex  $u \in DT$  where  $i \in \{0, 2, 4\}$ , such that  $\text{i-distant}(u, i)$  is true do
17    $v_{\text{next}} \leftarrow \text{first}(u, i + 1)$ ;
18    $v_{\text{prev}} \leftarrow \text{last}(u, i - 1)$ ;
19   Add edge  $\{v_{\text{next}}, v_{\text{prev}}\}$  to  $E$ ;
20    $\text{charge}(v_{\text{next}}, i + 1) \leftarrow \text{charge}(v_{\text{next}}, i + 1) + 1$ ;
21    $\text{charge}(v_{\text{prev}}, i - 1) \leftarrow \text{charge}(v_{\text{prev}}, i - 1) + 1$ ;
22   Let  $v_{\text{remove}}$  be the vertex from  $v_{\text{next}}, v_{\text{prev}}$  where  $\angle(\text{parent}(u, i), u, v_{\text{remove}})$  is maximized;
23   Remove edge  $\{u, v_{\text{remove}}\}$  from  $E$ ;
24    $\text{charge}(u, i) \leftarrow \text{charge}(u, i) - 1$ ;
25 end
26 foreach cone  $i$  of vertex  $u \in DT$  where  $i \in \{0, 1, \dots, 5\}$ , such that  $\text{charge}(u, i) = 2 \wedge \text{charge}(u, i - 1) = 1 \wedge$ 
    $\text{charge}(u, i + 1) = 1$  do
27   if  $u = \text{last}(\text{parent}(u, i), i)$  then
28      $v_{\text{remove}} \leftarrow \text{last}(u, i - 1)$ ;
29   else
30      $v_{\text{remove}} \leftarrow \text{first}(u, i + 1)$ ;
31   end
32   Remove edge  $\{u, v_{\text{remove}}\}$  from  $E$ ;
33    $\text{charge}(u, i) \leftarrow \text{charge}(u, i) - 1$ ;
34 end
35 return  $E$ ;
```

Algorithm 10: $\text{i-relevant}(v, u, i)$

1 $w \leftarrow \text{parent}(u, i)$;
2 **return** $v \neq \text{closest}(u, i) \wedge v \in C_w^i$;

Algorithm 11: $\text{i-distant}(w, i)$

1 $u \leftarrow \text{parent}(w, i)$;
2 **return** $\{w, u\} \notin E \wedge \text{i-relevant}(\text{first}(w, i + 1), u, i + 1) \wedge \text{i-relevant}(\text{last}(w, i - 1), u, i - 1)$;

Algorithm 12: $\text{parent}(u, i)$

1 **return** the closest vertex to u in a even cone i , if it exists;

Algorithm 13: $\text{closest}(u, i)$

1 **return** the closest vertex to u in a odd cone i , if it exists;

Algorithm 14: $\text{first}(u, i)$

1 **return** the first vertex in a odd cone i , if it exists;

Algorithm 15: $\text{last}(u, i)$

1 **return** the last vertex in a odd cone i , if it exists;

Algorithm 16: $\text{charge}(u, i)$

1 **return** the number of edges charged to cone i of u ;

Algorithm 17: $\text{KPX10}(P, \text{integer } k \geq 14)$

1 $DT \leftarrow L_2\text{-DelaunayTriangulation}(P)$;
2 **foreach** vertex $u \in DT$ **do**
3 Partition the area surrounding u into k disjoint cones of angle $2\pi/k$;
4 In each nonempty cone, **select** the shortest edge in DT incident to u ;
5 **foreach** maximal sequence of $\ell \geq 1$ consecutive empty cones **do**
6 **if** $\ell > 1$ **then**
7 **select** the first $\lfloor \ell/2 \rfloor$ **unselected** incident DT edges on u clockwise from the sequence of empty cones and the first $\lceil \ell/2 \rceil$ **unselected** DT edges incident on u counterclockwise from the sequence of empty cones;
8 **else**
9 let ux and uy be the incident DT edges on u clockwise and counterclockwise, respectively, from the empty cone;
10 **if** either ux or uy is selected then **select** the other edge (in case it has not been selected); otherwise **select** the shorter edge between ux and uy breaking ties arbitrarily;
11 **end**
12 **end**
13 **end**
14 **return** the DT edges selected by both endpoints;

- **KX12: Kanj and Xia [34]**. This $O(n \log n)$ -time algorithm takes a different approach in contrast with the previous ones, although it still uses the L_2 -Delaunay triangulation DT as the starting point. Every vertex u in DT selects at most 11 of its incident edges in DT , and edges that are selected by both endpoints are kept. As such, it is guaranteed that the degree of the resulting subgraph is at most 11. The stretch factors of the generated spanners is shown to be at most $1.998 \left(\frac{2 \sin(2\pi/5) \cos(\pi/5)}{2 \sin(2\pi/5) \cos(\pi/5) - 1} \right) \approx 5.7$. Refer to Algorithm 18.
- **BCC12-7, BCC12-6: Bose, Carmi, and Chaitman-Yerushalmi [12]**. The authors present two algorithms in their paper. Whereas previous algorithms used strategies involving iterating over the vertices one-by-one, this algorithm takes the approach of iterating over the edges of the Delaunay triangulation in order of non-decreasing length to query agreement among the vertices for bounding degrees. **BCC12-7**, the simpler of the two, produces $1.998(1 + \sqrt{2})^2 \approx 11.6$ -spanners with degree 7. **BCC12-6**, on the other hand, constructs $11.998 \left(\frac{1}{1 - \tan(\pi/7)(1 + 1/\cos(\pi/14))} \right) \approx 81.7$ -spanners with degree 6 but not all edges come from the L_2 -Delaunay triangulation. Both these algorithms run in $O(n \log n)$ time. See Algorithm 19. The parameter $\Delta \in \{7, 6\}$ is used to control the degree. Depending on Δ , either Algorithm 21 or Algorithm 20 is invoked.

Algorithm 18: KX12(P)

```

1  $DT \leftarrow L_2\text{-DelaunayTriangulation}(P)$ ;
2 foreach vertex  $u \in DT$  do
3   In each wide sequence (a sequence of exactly three consecutive edges incident to a vertex whose overall
   angle is at least  $4\pi/5$ ) around  $u$ , select the edges of the sequence;
4   Partition the remaining space surrounding  $u$  not in a wide sequence into a minimum number of disjoint
   cones of maximum angle  $\pi/5$ ;
5   In each nonempty cone, select the shortest edge incident to  $u$ ;
6   In each empty cone, let  $ux$  and  $uy$  be the incident  $DT$  edges on  $u$  clockwise and counterclockwise,
   respectively, from the empty cone;
7   If either  $ux$  or  $uy$  is selected then select the other edge (in case it has not been selected); otherwise
   select the longer edge between  $ux$  and  $uy$  breaking ties arbitrarily;
8 end
9 return all edges selected by both incident vertices;
```

Algorithm 19: BCC12($P, \Delta \in \{6, 7\}$)

```

1  $DT \leftarrow L_2\text{-DelaunayTriangulation}(P)$ ;
2  $E, E^* \leftarrow \emptyset$ ;
3 Initialize  $k = \Delta + 1$  cones surrounding each vertex  $u$ , oriented such that the shortest edge incident on  $u$  falls
   on a boundary;
4 foreach  $\{u, v\} \in DT$  in order of non-decreasing length do
5   if  $\forall C_u^i$  containing  $\{u, v\}$ ,  $C_u^i \cap E = \emptyset$  and  $\forall C_v^j$  containing  $\{u, v\}$ ,  $C_v^j \cap E = \emptyset$  then
6     | Add edge  $\{u, v\}$  to  $E$ ;
7   end
8 end
9 foreach  $\{u, v\} \in E$  do
10  |  $\text{Wedge}_\Delta(u, v)$ ;
11  |  $\text{Wedge}_\Delta(v, u)$ ;
12 end
13 return  $E \cup E^*$ ;
```

- **BKPX15: Bonichon, Kanj, Perković, and Xia [11]**. This algorithm uses the L_∞ -Delaunay triangulation and was the first degree-4 algorithm. For such triangulations, empty axis parallel squares are used for characterization instead of empty circles, as needed in the case of L_2 -Delaunay triangulations. The L_∞ -distance between two points u, w is defined as $d_\infty(u, w) = \max(d_x(u, w), d_y(u, w))$. From the L_∞ -Delaunay

Algorithm 20: Wedge₇(u, v_i)

```
1 foreach  $C_u^z$  containing  $\{u, v_i\}$  do
2   Let  $\{u, v_j\}$  and  $\{u, v_k\}$  be the first and last edges of  $DT$  in the cone;
3   Add all edges  $\{v_m, v_{m+1}\}$  to  $E^*$  such that  $j < m < i - 1$  or  $i < m < k - 1$ ;
4   if  $\{u, v_{i+1}\} \in C_u^z$  and  $v_{i+1} \neq v_k$  and  $\angle uv_i v_{i+1} > \pi/2$  then
5     | Add edge  $\{v_i, v_{i+1}\}$  to  $E^*$ ;
6   end
7   if  $\{u, v_{i-1}\} \in C_u^z$  and  $v_{i-1} \neq v_k$  and  $\angle uv_i v_{i-1} > \pi/2$  then
8     | Add edge  $\{v_i, v_{i-1}\}$  to  $E^*$ ;
9   end
10 end
```

Algorithm 21: Wedge₆(u, v_i)

```
1 foreach  $C_u^z$  containing  $\{u, v_i\}$  do
2   Let  $Q = \{v_n : \{u, v_n\} \in C_u^z \cap DT\} = \{v_j, \dots, v_k\}$ ;
3   Let  $Q' = \{v_n : \angle v_{n-1} v_n v_{n+1} < 6\pi/7, v_n \in Q \setminus \{v_j, v_i, v_k\}\}$ ;
4   Add all edges  $\{v_n, v_{n+1}\}$  to  $E^*$  such that  $v_n, v_{n+1} \notin Q'$  and  $n \in [j+1, i-2] \cup [i+1, k-2]$ ;
   /* W.l.o.g. the points of  $Q'$  lie between  $v_i$  and  $v_k$  (the symmetric case is handled
   analogously) */
5   if  $\angle uv_i v_{i-1} > 4\pi/7$  and  $i, i-1 \neq j$  then
6     | Add edge  $\{v_i, v_{i-1}\}$  to  $E^*$ ;
7   end
8   Let  $v_f$  be the first point in  $Q'$ ;
9   Let  $a = \min\{n | n > f \text{ and } v_n \in Q \setminus Q'\}$ ;
10  if  $f = i+1$  then
11    | if  $\angle uv_i v_{i+1} \leq 4\pi/7$  and  $a \neq k$  then
12      | Add edge  $\{v_f, v_a\}$  to  $E^*$ ;
13    | end
14    | if  $\angle uv_i v_{i+1} > 4\pi/7$  and  $f+1 \neq k$  then
15      | Add edge  $\{v_i, v_{f+1}\}$  to  $E^*$ ;
16    | end
17  else
18    | Let  $v_\ell$  be the last point in  $Q'$ ;
19    | Let  $b = \max\{n | n < \ell \text{ and } v_n \in Q \setminus Q'\}$ ;
20    | if  $\ell = k-1$  then
21      | Add edge  $\{v_\ell, v_b\}$  to  $E^*$ ;
22    | else
23      | Add edge  $\{v_b, v_{\ell+1}\}$  to  $E^*$ ;
24      | if  $v_{\ell-1} \in Q'$  then
25        | Add edge  $\{v_\ell, v_{\ell-1}\}$  to  $E^*$ ;
26      | end
27    | end
28  end
29 end
```

triangulation, a directed L_∞ -distance-based Yao graph $\overrightarrow{Y}_4^\infty$ is constructed that is a plane $\sqrt{20 + 14\sqrt{2}}$ -spanner. Then a degree-8 subgraph H_8 of Y_4^∞ is constructed. Finally, some redundant edges are removed and new shortcut edges are added to obtain the final plane degree-4 spanner with a stretch factor of $\sqrt{20 + 14\sqrt{2}}(19 + 29\sqrt{2}) \approx 156.8$. No runtime analysis is presented by the authors. Refer to Algorithm 29. The algorithm divides the space around each point into 4 cones, separated by the x and y -axes after translating the point to the origin. Each cone has an associated **charge**, which can be 0, 1, or 2. The algorithm labels certain edges as follows. Each edge will be an **anchor** or a **non-anchor** and **weak** or **strong**. Further, each edge may have an additional label of **start-of-odd-chain-anchor**. A **weak anchor chain** is a path $w_0, w_1, w_2, \dots, w_k$ of maximal length consisting of **weak anchors** such that the cone of each edge (wrt the source vertex) alternates between some i and $i + 2$. **Canonical** edges are edges between consecutive vertices in the ordered neighborhood of a vertex u in a common cone i . An edge (u, v) is said to be **dual** if there are two or more edges of $\overrightarrow{Y}_4^\infty$ incident to cone i of u and cone $i + 2$ of v .

Algorithm 22: `constructYaoInfinityGraph(DT)`

```

1  $\overrightarrow{Y}_4^\infty \leftarrow \emptyset;$ 
2 foreach  $u \in DT$  do
3   foreach  $C_u^i$  do
4     Let  $v \in C_u^i$  be the vertex with the smallest  $L_\infty$  distance;
5     Add  $(u, v)$  to  $\overrightarrow{Y}_4^\infty;$ 
6   end
7 end
8 return  $\overrightarrow{Y}_4^\infty;$ 

```

- **KPT17: Kanj, Perković, and Türkoğlu [32].** Akin to BGHP10, this algorithm uses the *TD*-Delaunay triangulation and Θ -graph to introduce fresh techniques in spanner construction. Refer to Algorithm 30 for a pseudocode of this algorithm. The authors show that their algorithm generates degree-4 spanners with a stretch factor of 20 and runs in $O(n \log n)$ time. In the following, we define the notations used in the pseudocode.
 - For each vertex, the shortest edge in each odd cone is called an anchor.
 - Cones 1 and 4 are labelled as **blue** and the rest as **white**.
 - The first and last edges incident upon a vertex u in a cone i are called the **boundary** edges of u in i .
 - The **canonical** path is made up of all **canonical** edges incident on u in cone i , forming a path from one **boundary** edge in the cone to the other.
- **BHS18: Bose, Hill, and Smid [14].** This algorithm produces a plane degree-8 spanner with stretch factor at most $1.998 \left(1 + \frac{2\pi}{6 \cos(\pi/6)}\right) \approx 4.4$ using the L_2 -Delaunay triangulation and Θ -graph. However, the authors do not present any runtime analysis of their algorithm. In BHS18, the space around every point p is divided into six cones and are oriented such that a boundary lies on the x -axis after translating p to the origin. The algorithm starts with the L_2 -Delaunay triangulation DT , then, in order of non-decreasing bisector distance, each edge is added to the spanner if the cones containing it are both empty. For each edge added here, certain *canonical* edges will also be carefully added to the spanner. Refer to Algorithm 31. In the following, we define the notations used in this pseudocode.
 - The **bisector-distance** $[pq]$ between p and q is the distance from p to the orthogonal projection of q onto the bisector of C_i^p where $q \in C_i^p$.
 - Let $\{q_0, q_1, \dots, q_{d-1}\}$ be the sequence of all neighbors of p in DT in consecutive clockwise order. The neighborhood N_p with apex p is the graph with the vertex set $\{p, q_0, q_1, \dots, q_{d-1}\}$ and the edge set $\{\{q_j, q_{j+1}\}\} \cup \{\{q_j, q_{j+1}\}\}, 0 \leq j \leq d - 1$, with all values mod d . The edges $\{\{q_j, q_{j+1}\}\}$ are called *canonical edges*.

Algorithm 23: $\text{selectAnchors}(\overrightarrow{Y_4^\infty}, DT)$

```
1 foreach  $(u, v) \in \overrightarrow{Y_4^\infty}$  do
2   Let  $i$  be the cone of  $u$  containing  $v$ ;
3    $v_{\text{anchor}} \leftarrow v$ ;
4   if  $\neg \text{isMutuallySingle}(\overrightarrow{Y_4^\infty}, u, v, i)$  and  $u$  has more than one  $\overrightarrow{Y_4^\infty}$  edge in  $C_u^i$  then
5     Let  $\ell$  be the position of  $v$  and  $k$  the number of vertices in  $\text{fan}(DT, u, i)$ ;
6     if  $\ell \geq 2$  and  $(v_{\ell-1}, v_\ell) \in \overrightarrow{Y_4^\infty}$  and  $(v_\ell, v_{\ell-1}) \notin \overrightarrow{Y_4^\infty}$  then
7       Let  $v_{\ell'}$  such that  $\ell' < \ell$  be the starting vertex of the maximal unidirectional canonical path
8         ending at  $v_\ell$ ;
9        $v_{\text{anchor}} \leftarrow v_{\ell'}$ ;
10    else if  $\ell \leq k - 1$  and  $(v_{\ell+1}, v_\ell) \in \overrightarrow{Y_4^\infty}$  and  $(v_\ell, v_{\ell+1}) \notin \overrightarrow{Y_4^\infty}$  then
11      Let  $v_{\ell'}$  such that  $\ell' > \ell$  be the starting vertex of the maximal unidirectional canonical path
12        ending at  $v_\ell$ ;
13       $v_{\text{anchor}} \leftarrow v_{\ell'}$ ;
14    end
15    Mark  $(u, v_{\text{anchor}})$  as the anchor of  $C_u^i$ ;
16  end
17   $A \leftarrow \emptyset$ ;
18  foreach anchor  $(u, v)$  in each  $C_u^i$  do
19    if anchor of  $C_v^{i+2}$  is  $(v, u)$  or undefined then
20      Mark  $(u, v)$  as strong and add it to  $A$ ;
21    else
22      Mark  $(u, v)$  as weak;
23    end
24  end
25  foreach weak anchor  $(u, v)$  in each  $C_u^i$  do
26    if  $u$  begins the weak anchor chain  $(w_0, w_1, \dots, w_k)$  then
27      if  $k$  is odd then
28        Mark  $(w_0, w_1)$  as a start-of-odd-chain-anchor;
29      end
30      for  $\ell = k - 1$ ;  $\ell \geq 0$ ;  $\ell = \ell - 2$  do
31        Add  $(w_{\ell-1}, w_\ell)$  to  $A$ ;
32      end
33    end
34  end
35  return  $A$ ;
```

Algorithm 24: $\text{fan}(DT, u, i)$

```
1 return all neighboring vertices  $(v_1, v_2, \dots, v_k)$  in  $C_u^i$  in counterclockwise order;
```

Algorithm 25: $\text{isMutuallySingle}(\overrightarrow{Y_4^\infty}, u, v, i)$

```
1 return  $u$  has one  $\overrightarrow{Y_4^\infty}$  edge in  $C_u^i$  and  $v$  has one  $\overrightarrow{Y_4^\infty}$  edge in  $C_v^{i+2}$ ;
```

Algorithm 26: $\text{degree8Spanner}(A, \overrightarrow{Y_4^\infty}, DT)$

```
1 Charge each anchor  $(u, v) \in A$  to the cones of each vertex in which the edge lies;
2  $H_8 \leftarrow A$ ;
3 foreach vertex  $u$  and cone  $i$  of  $u$  do
4    $\{v_1, \dots, v_k\} \leftarrow \text{fan}(DT, u, i)$ ;
5   if  $k \geq 2$  then
6     Add all uni-directional canonical edges to  $H_8$  except  $(v_2, v_1)$  and  $(v_{k-1}, v_k)$ ;
7     if  $(v_2, v_1)$  is a non-anchor, uni-directional edge such that  $(v_2, v_1) \in \overrightarrow{Y_4^\infty} \wedge (v_1, v_2) \notin \overrightarrow{Y_4^\infty} \wedge (v_1, u)$  is a
      dual edge  $\wedge$  not a start-of-odd-chain anchor chosen by  $v_1$  then
8       | Add  $(v_2, v_1)$  to  $H_8$ ;
9     end
10    if  $(v_{k-1}, v_k)$  is a non-anchor, uni-directional edge such that
       $(v_{k-1}, v_k) \in \overrightarrow{Y_4^\infty} \wedge (v_k, v_{k-1}) \notin \overrightarrow{Y_4^\infty} \wedge (v_k, u)$  is a dual edge  $\wedge$  not a start-of-odd-chain anchor
      chosen by  $v_k$  then
11      | Add  $(v_{k-1}, v_k)$  to  $H_8$ ;
12    end
13    foreach canonical edge  $(v, w)$  added to  $H_8$  do
14       $v_{\text{charge}} \leftarrow v$ ;
15      if  $(v, w)$  is a non-anchor then
16        |  $v_{\text{charge}} \leftarrow u$ ;
17      end
18      Charge  $(v, w)$  to the cone of  $v$  containing  $w$  and the cone of  $w$  containing  $v_{\text{charge}}$ ;
19    end
20  end
21 end
22 return  $H_8$ ;
```

Algorithm 27: $\text{processDupEdgeChains}(H_8, \overrightarrow{Y_4^\infty})$

```
1  $H_6 \leftarrow H_8$ ;
2 foreach uni-directional non-anchor  $(u, v)$  in cone  $i$  of  $u$  in  $H_8$  with charge = 1 do
3   if cone  $i+1$  or  $i-1$  of  $v$  has charge = 2  $\wedge (u, v)$  is charged to cone  $i+1$  or  $i-1$  of  $v$  then
4     Let  $j$  be the cone of  $v$  where  $(u, v)$  is charged;
5      $v_{\text{current}} \leftarrow u, v_{\text{next}} \leftarrow v, D \leftarrow \emptyset$ ;
6     while cone  $j$  of  $v_{\text{next}}$  has charge = 2  $\wedge (v_{\text{current}}, v_{\text{next}})$  is in cone  $j$  of  $v_{\text{next}}$  do
7       | Add  $(v_{\text{current}}, v_{\text{next}})$  to  $D$ ;
8       |  $v_{\text{current}} \leftarrow v_{\text{next}}$ ;
9       | Set  $v_{\text{next}}$  to the target of the  $\overrightarrow{Y_4^\infty}$  edge beginning in cone  $j$  of  $v_{\text{current}}$ ;
10      | swap( $i, j$ );
11    end
12    Starting with the last edge in the path induced by  $D$ , remove every other edge from  $H_6$ ;
13  end
14 end
15 return  $H_6$ ;
```

Algorithm 28: $\text{createShortcuts}(H_6, \overrightarrow{Y_4^\infty}, DT)$

```
1  $H_4 \leftarrow H_6$ ;  
2 foreach pair of non-anchor uni-directional canonical edges  $(v_{r-1}, v_r), (v_{r+1}, v_r)$  in cone  $i$  of  $u$  do  
3   Remove  $(v_{r-1}, v_r)$  and  $(v_{r+1}, v_r)$  from  $H_4$ ;  
4   Add  $(v_{r-1}, v_{r+1})$  to  $H_4$ ;  
5   Charge this edge to the cones of each vertex in which the edge lies;  
6 end  
7 return  $H_4$ ;
```

Algorithm 29: $\text{BKPX15}(P)$

```
1  $DT \leftarrow L_\infty\text{-DelaunayTriangulation}(P)$ ;  
2  $\overrightarrow{Y_4^\infty} \leftarrow \text{constructYaoInfinityGraph}(DT)$  (Algorithm 22);  
3  $A \leftarrow \text{selectAnchors}(\overrightarrow{Y_4^\infty}, DT)$  (Algorithm 23);  
4  $H_8 \leftarrow \text{degree8Spanner}(A, \overrightarrow{Y_4^\infty}, DT)$  (Algorithm 26);  
5  $H_6 \leftarrow \text{processDupEdgeChains}(H_8, \overrightarrow{Y_4^\infty})$  (Algorithm 27);  
6  $H_4 \leftarrow \text{createShortcuts}(H_6, \overrightarrow{Y_4^\infty}, DT)$  (Algorithm 28);  
7 return  $H_4$ ;
```

- N_i^p is the subgraph of N_p induced by all the vertices of N_p in C_i^p , including p .
- Let $\text{Can}_i^{\{p,r\}}$ be the subgraph of DT consisting of the ordered subsequence of canonical edges $\{s, t\}$ of N_i^p in clockwise order around apex p such that $[ps] \geq [pr]$ and $[pt] \geq [pr]$.

3 Estimating stretch factors of large spanners

Measuring exact stretch factors of large graphs is a tedious job, and so is for geometric spanners. Although many algorithms exist in the literature for constructing geometric spanners, nothing is known about practical algorithms for computing stretch factors of large geometric spanners. It is a severe bottleneck for conducting experiments with large spanners since the stretch factor is considered a fundamental quality of geometric spanners.

For any spanner (not necessarily geometric) on n vertices, its exact stretch factor can be computed in $O(n^3 \log n)$ time by running the folklore Dijkstra algorithm (implemented using a Fibonacci heap) from every vertex, and in $\Theta(n^3)$ time by running the classic Floyd-Warshall algorithm. Note that the Dijkstra-based algorithm runs $O(n^2 \log n)$ time for plane spanners since the number of edges is $O(n)$. Both of these are very slow in practice. However, the latter has a quadratic space-complexity and is unusable when n is large. Consequently, they are practically useless when n is large. Stretch factor estimation of large geometric graphs appears to be a far cry despite theoretical studies on this problem; refer to [2, 20, 28, 38, 43]. We believe these algorithms are either involved from an algorithm engineering standpoint or rely on well-separated pair decomposition [18], which may potentially slow down practical implementations due to the large number of well-separated pairs needed by those algorithms. This has motivated us to design a practical algorithm, named APPXSTRETCHFACTOR, that gives a lower-bound on the actual stretch factor of any geometric spanner (not necessarily plane). However, we will consider the universe of plane geometric spanners as the input domain in this work. To our knowledge, we are not aware of any such algorithm in the literature. Refer to Algorithm 34. It takes as input an n -element pointset P and a geometric graph G , constructed on P .

The underlying idea of our algorithm is as follows. We observe that most geometric spanners are well-constructed; meaning it is likely that far away points (having many hops in the shortest paths between them) have low detour ratios (ratio of the length of a shortest path to that of the Euclidean distance) between them and the worst-case detour is achieved by point pairs that are a few hops apart. Note that stretch factor of

Algorithm 30: KPT17(P)

```
1  $DT \leftarrow \text{TD-DelaunayTriangulation}(P)$ ;  
2  $E, A \leftarrow \emptyset$ ;  
3 foreach white anchor  $(u, v)$  in increasing order of  $d_v$  length do  
4   | if  $u$  and  $v$  do not have a white anchor in a cone adjacent to  $(u, v)$ 's cone then  
5   |   | Add  $(u, v)$  to  $A$ ;  
6   |   end  
7 end  
8 Add all blue anchors to  $A$ ;  
9 foreach blue anchor  $u$  do  
10  | Let  $s_1, s_2, \dots, s_m$  be the clockwise ordered neighbors of  $u$  in  $DT$ ;  
11  | Add all canonical edges  $(s_\ell, s_{\ell+1}) \notin A$  to  $E$  such that  $1 \leq \ell < m$ ;  
12 end  
13 foreach pair of canonical edges  $(u, v), (w, v) \in E$  in a blue cone do  
14  | Remove  $(u, v)$  and  $(w, v)$  from  $E$ ;  
15  | Add a shortcut edge  $(u, w)$  to  $E$ ;  
16 end  
17 foreach white canonical edge  $(u, v)$  on the white side of its anchor  $a$  do  
18  | if  $a \notin A$  then  
19  |   | Add  $(u, v)$  to  $E$ ;  
20  |   end  
21 end  
22 foreach white anchor  $(v, w)$  and its boundary edge  $(u, w) \neq (v, w)$  on the white side do  
23  | Let  $u = s_1, s_2, \dots, s_m = v$  be the canonical path between  $u$  and  $v$ ;  
24  | for  $i = 0$  to  $m$  do  
25  |   | if  $(s_{i+1}, s_i)$  is blue then  
26  |     | Let  $j$  be the smallest index in  $P_i = \{s_{i+1}, \dots, s_m\}$  such that  $s_j$  is in a white cone of  $s_i$  and  $P_i$  lies  
27  |     |   on the same side (or on) the straight line  $s_i s_j$ ;  
28  |     | Add the shortcut  $(s_j, s_i)$  to  $E$ ;  
29  |     | if  $(s_j, s_{j-1}) \in E$  then  
30  |     |   | Remove  $(s_j, s_{j-1})$  from  $E$ ;  
31  |     |   end  
32  |     |  $i \leftarrow j$ ;  
33  |     | end  
34 end  
35 return  $E \cup A$ ;
```

Algorithm 31: BHS18(P)

```
1  $DT \leftarrow L_2\text{-DelaunayTriangulation}(P)$ ;  
2 Let  $m$  be the number of edges in  $DT$ ;  
3  $L$  be the edges  $\in DT$  sorted in non-decreasing order of bisector-distance;  
4  $E_A \leftarrow \text{addIncident}(L)$ ,  $E_{CAN} \leftarrow \emptyset$ ;  
5 foreach  $\{u, v\} \in E_A$  do  
6  |  $E_{CAN} \leftarrow E_{CAN} \cup \text{addCanonical}(u, v) \cup \text{addCanonical}(v, u)$ ;  
7 end  
8 return  $E_A \cup E_{CAN}$ ;
```

Algorithm 32: addIncident(L)

```
1  $E_A \leftarrow \emptyset$ ;  
2 foreach  $\{u, v\} \in L$  do  
3   | Let  $i$  be the cone of  $u$  containing  $v$ ;  
4   | if  $\{u, w\} \notin E_A$  for all  $w \in N_i^u \wedge \{v, y\} \notin E_A$  for all  $y \in N_{i+3}^v$  then  
5   |   | Add  $\{u, v\}$  to  $E_A$ ;  
6   | end  
7 end  
8 return  $E_A$ ;
```

Algorithm 33: addCanonical(u, v)

```
1  $E' \leftarrow \emptyset$ ;  
2 Let  $i$  be the cone of  $u$  containing  $v$ ;  
3 Let  $e_{first}$  and  $e_{last}$  be the first and last canonical edge in  $Can_i^{\{u, v\}}$ ;  
4 if  $Can_i^{\{u, v\}}$  has at least 3 edges then  
5   | foreach  $\{s, t\} \in Can_i^{\{u, v\}} \setminus \{e_{first}, e_{last}\}$  do  
6   |   | Add  $\{s, t\}$  to  $E'$ ;  
7   | end  
8 end  
9 if  $v \in \{e_{first}, e_{last}\}$  and there is more than one edge in  $Can_i^{\{u, v\}}$  then  
10 | Add the edge of  $Can_i^{\{u, v\}}$  incident to  $v$  to  $E'$ ;  
11 end  
12 foreach  $\{y, z\} \in \{e_{first}, e_{last}\}$  do  
13 | if  $\{y, z\} \in N_{i-1}^z$  then  
14 |   | Add  $\{y, z\}$  to  $E'$ ;  
15 | end  
16 | if  $\{y, z\} \in N_{i-2}^z$  then  
17 |   | if  $N_{i-2}^z \cap E_A$  does not have an edge incident to  $z$  then  
18 |   |   | Add  $\{y, z\}$  to  $E'$ ;  
19 |   | end  
20 |   | if  $N_{i-2}^z \cap E_A \setminus \{y, z\}$  has an edge incident to  $z$  then  
21 |   |   | Let  $\{w, y\}$  be the canonical edge of  $z$  incident to  $y$ ;  
22 |   |   | Add  $\{w, y\}$  to  $E'$ ;  
23 |   | end  
24 | end  
25 end  
26 return  $E'$ ;
```

Algorithm 34: APPXSTRETCHFACTOR(P, G)

```
1  $DT \leftarrow L_2$ -DelaunayTriangulation( $P$ );
2  $t \leftarrow 1$ ;
3 foreach  $p \in P$  do
4    $h \leftarrow 1, t_p \leftarrow 1$ ;
5   while true do
6     Let  $X$  denote the set of points which are exactly  $h$  hops away from  $p$  in  $DT$  found using a
       breadth-first traversal originating at  $u$ ;
7      $t' \leftarrow 1$ ;
8     foreach  $q \in X$  do
9        $t' \leftarrow \max\left(\frac{|\pi_G(p,q)|}{|pq|}, t'\right)$ ;
10    end
11    if  $t' > t_p$  then
12       $h \leftarrow h + 1; t_p \leftarrow t'$ ;
13    else
14      break;
15    end
16     $t \leftarrow \max(t, t_p)$ ;
17 end
18 return  $t$ ;
```

a graph is the maximum detour ratio over all vertex pairs. To capture *closeness*, we use the L_2 -Delaunay triangulation constructed on P as the basis. For every point $p \in P$, we start a breadth-first traversal on the Delaunay triangulation DT . At every level, we compute the detour ratios in G from p to all the points in that level. If a worse detour ratio is found in the current level compared to the worst found in the previous level, we continue to the next level; otherwise, the process is terminated. For finding detour ratios in G , we use the folklore Dijkstra algorithm since computation of shortest paths are required. In our algorithm, $\pi_G(p, q)$ denotes a shortest path between the points $p, q \in P$ in G and $|\pi_G(p, q)|$ its total length. The detour between p, q in G can be easily calculated as $|\pi_G(p, q)|/|pq|$. The current level is denoted by h . It is assumed that the neighbors of p in G are at level 1. For efficiency reasons, we do not restart the Dijkstra at every level of the breadth-first traversal; instead, we save our progress from the previous level and continue after that.

To our surprise, we find that for the class of spanners used in this work, APPXSTRETCHFACTOR returned exact stretch factors almost every time. The precision error was very low whenever it failed to compute the exact stretch factor. Further, our algorithm can be parallelized very easily by spawning parallel iterations of the **foreach** loop. Apart from the L_2 -Delaunay triangulation (which can be constructed very fast in practice), it does not use any advanced geometric structure, making it fast in practice. We present our experimental observations for this algorithm in Section 4.3.

4 Experiments

We have implemented the algorithms in GNU C++17 using the CGAL library [41]. The machine used for experiments is equipped with a AMD Ryzen 5 1600 (3.2 GHz) processor and 24 GB of main memory, and runs Ubuntu Linux 20.04 LTS. The g++ compiler was invoked with -O3 flag to achieve fast real-world speed. From CGAL, the Exact_predicates_inexact_constructions_kernel is used for accuracy and speed. We have tried our best to tune our codes to run fast.

All the eleven algorithms considered in this work use one of the following three kinds of Delaunay triangulation as the starting point: L_2 , TD , and L_∞ . For constructing L_2 and L_∞ -Delaunay triangulations, the CGAL::Delaunay_triangulation_2 and CGAL::Segment_Delaunay_graph_Linf_2 implementations have been used, respectively. As of now, a TD -Delaunay triangulation implementation is not available in the CGAL. It was pointed out by Chew in [22] that such triangulations can be constructed in $O(n \log n)$ time. However,

no precise implementable algorithm was presented. But luckily, it is shown in [8] by Bonichon et al. that TD -Delaunay triangulation of a pointset is same as its $\frac{1}{2}$ - Θ graph. We leveraged this result and used the $O(n \log n)$ time `CGAL::Construct_theta_graph_2` implementation for constructing the TD -Delaunay triangulations. For faster speed, the input pointsets are always sorted using `CGAL::spatial_sort` before constructing Delaunay triangulations on them. We share the implementations via [GitHub](#)⁵.

In our experiments, we have used both synthetic and real-world pointsets, as described next.

4.1 Synthetic pointsets

We have used the following eight distributions to generate synthetic pointsets for our experiments. The selection of these distributions are inspired by the ones used in [5, 29, 30, 40] for geometric experiments. See Figure 2 to visualize these eight distributions.

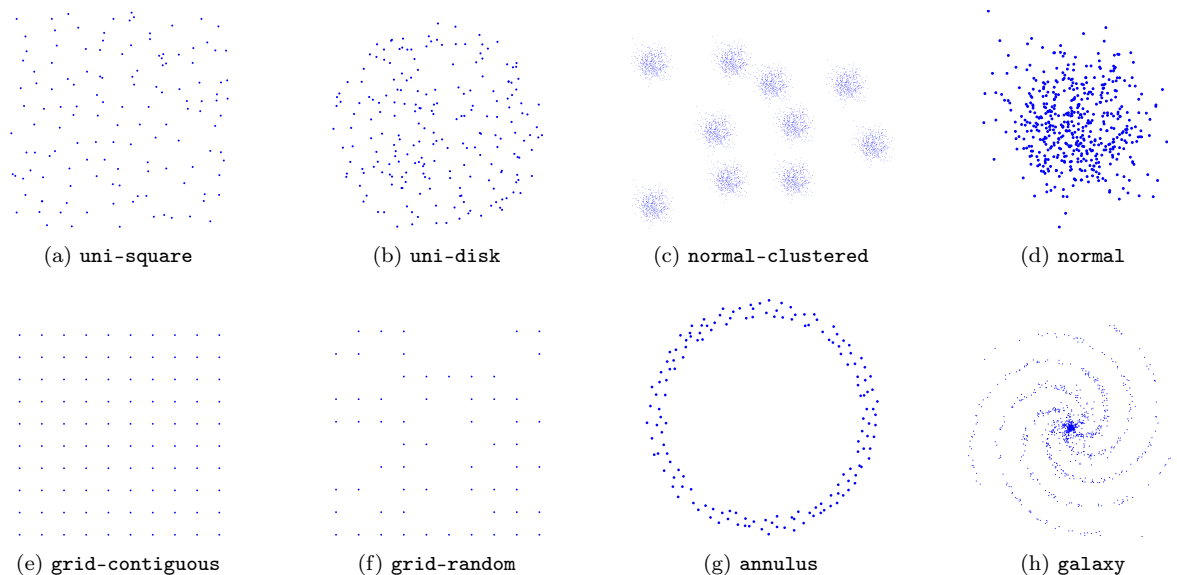


Figure 2: The eight distributions used to generate synthetic pointsets for our experiments.

- (a) **uni-square**. Points are generated uniformly inside a square of side length of 1000 using the `CGAL::Random_points_in_square` generator.
- (b) **uni-disk**. Points are generated uniformly inside a disc of radius 1000 using the `CGAL::Random_points_in_disc_2` generator.
- (c) **normal-clustered**. A set of 10 normally distributed clusters placed randomly in the plane. Each cluster contains $n/10$ normally distributed points (mean and standard-deviation are set to 2.0). We have used `std::normal_distribution<double>` to generate the point coordinates.
- (d) **normal**. This is same as **normal-clustered** except that only one cluster is used.
- (e) **grid-contiguous**. Points are generated contiguously on a $\lceil \sqrt{n} \rceil \times \lceil \sqrt{n} \rceil$ square grid using the `CGAL::points_on_square_grid_2` generator.
- (f) **grid-random**. Points are generated on a $\lceil 0.7n \rceil \times \lceil 0.7n \rceil$ unit square grid. The value 0.7 is chosen arbitrarily to obtain well-separated non-contiguous grid points. The coordinates of the generated points are integers and are generated independently using `std::uniform_int_distribution`.
- (g) **annulus**. Points are generated inside an annulus whose outer radius is set to 1000 and the inner-radius is set to 800. The coordinates are generated using `std::uniform_real_distribution`.

⁵<https://github.com/ghoshanirban/BoundedDegreePlaneSpannersCppCode>

(h) `galaxy`. Points are generated in the shape of a spiral galaxy having outer five arms; see [31].

For seeding the random number generators from C++, we have used the Mersenne twister engine `std::mt19937`. Since some of the algorithms assume that no two points must have the same value x or y -coordinates, the generated pointsets have been perturbed using the `CGAL::perturb_points_2` function with 0.0001, 0.0001 as the two required parameters.

4.2 Real-world pointsets

The following real-world pointsets are obtained from various publicly available sources. We have removed duplicate points (wherever present) from the pointsets. The main reason behind the use of such pointsets is that they do not follow the popular synthetic distributions. Hence, experimenting with them is beneficial to see how the algorithms perform on them.

- `burma` [1]. An 33,708-element pointset representing cities in Burma.
- `birch3` [17,30]. An 99,801-element pointset representing random clusters at random locations.
- `monalisa` [1,30]: A 100,000-city TSP instance representing a continuous-line drawing of the Mona Lisa.
- `KDDCU2D` [17,30]. An 104,297-element pointset representing the first two dimensions of a protein data-set.
- `usa` [1,30]. A 115,475-city TSP instance representing (nearly) all towns, villages, and cities in the United States.
- `europa` [17,30]. An 168,896-element pointset representing differential coordinates of the map of Europe.
- `wiki`⁶. An 317,695-element pointset of coordinates found in English-language Wikipedia articles.
- `vlsi` [1]. An 744,710-element pointset representing a Very Large Scale Integration chip.
- `china` [17,30]. An 808,693-element pointset representing cities in China.
- `uber`⁷. An 1,381,253-element pointset representing Uber pickup locations in New York City.
- `world` [1,30]. An 1,904,711-element pointset representing all locations in the world that are registered as populated cities or towns, as well as several research bases in Antarctica.

4.3 Efficacy of APPXSTRETCHFACTOR

We have seen in Section 3, it is quite challenging to measure stretch factor of large spanners. This motivated us to design and use the APPXSTRETCHFACTOR algorithm in our experiments for estimating stretch factors of the generated spanners. In the following, we compare APPXSTRETCHFACTOR with the Dijkstra’s algorithm (run from every vertex) and show that for the eight distributions it is not only much faster than Dijkstra but can also estimate stretch factors of plane spanners with high accuracy.

The main reason behind the fast practical performance of APPXSTRETCHFACTOR is early terminations of the breadth-first traversals (one traversal per vertex), which in turn makes Dijkstra run fast to find the shortest paths to the vertices in all the levels. We have noticed in our experiments that the pair that achieves the stretch factor for a bounded-degree plane spanner are typically a few hops away and pairwise stretch factors (ratio of detour between two vertices to that of their Euclidean distance) drop with the increase in hops. Consequently, the breadth-first traversals terminate very early most of the time.

The total number of pointsets used in this comparison experiment is $11 \cdot 8 \cdot 10 \cdot 5 = 4400$ since there are 11 algorithms, 8 distributions, 10 distinct values of n ($1K, 2K, \dots, 10K$), and 5 samples were used for every value of n . Out of these many, the number of times APPXSTRETCHFACTOR has failed to return the exact stretch factor is just 8. So, the observed failure rate is $\approx 0.18\%$. Interestingly, in the cases where APPXSTRETCHFACTOR failed to compute the exact stretch factor, the largest observed error percentage

⁶https://github.com/placemark/wiki_coordinates

⁷<https://www.kaggle.com/fivethirtyeight/uber-pickups-in-new-york-city>

between the exact stretch factor (found using Dijkstra) and the stretch factor returned by it is just ≈ 0.15 . This gives us the confidence that our algorithm can be safely used to estimate stretch factor of large spanners. Refer to the Figure 5. As evident from these graphs, APPXSTRETCHFACTOR is substantially faster than Dijkstra everywhere. Henceforth, we use APPXSTRETCHFACTOR (Algorithm 34) to estimate the stretch factors of the spanners in our experiments.

4.4 Experimental comparison of the algorithms

We compare the 11 implemented algorithms based on their runtimes and degree, stretch factor, and lightness⁸ of the generated spanners.

In the interest of space, we avoid legend tables everywhere in our plots. Since the legends are used uniformly everywhere, we present them here for an easy reference; see Fig. 3.

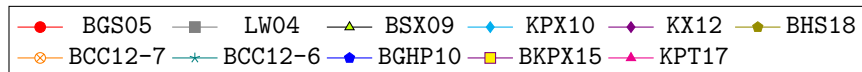


Figure 3: The plot legends.

For synthetic pointsets, we vary n from $10K$ to $100K$. For every value of n , we have used five random samples to measure runtimes and the above characteristics of the spanners. In the case of real-world pointsets, we run every one of them five times and report the average time taken.

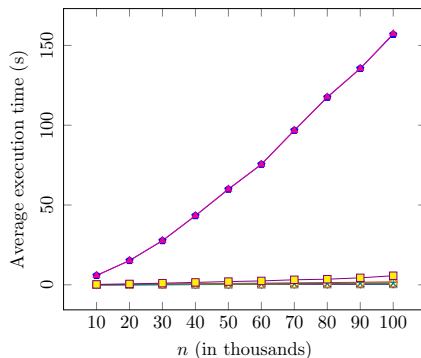


Figure 4: Points are generated using the `uni-square` distribution. For this particular experiment, n is in the range $10K, 20K, \dots, 100K$. The plots for BGHP10 and KPT17 have overlapped in this figure.

In our experiments, we find that BGHP10 and KPT17 are considerably slower than the other algorithms considered in this work. The reason behind this is slow construction of TD -Delaunay triangulations. Refer to Fig. 3 for an illustration. When $n = 100K$, both take more than 150 seconds to finish. In contrast, other nine algorithms take less than 10 seconds. Since real-world speed is an important factor for spanner construction algorithms, we do not consider them further in our runtime comparisons.

1. *Runtime.* Fast execution speed is highly desired for spanner construction on large pointsets. We present the runtimes for all eight distributions in the Fig. 6. As explained above, we have excluded BGHP10 and KPT17 from these plots since they are considerably slower than the other nine algorithms. Interestingly, we find that the relative performance of these algorithms is independent of the point distributions. For all the eight distributions, we find that BKPX15 is much slower than the others. This is mainly due to the time taken to construct L_∞ -Delaunay triangulations. Among the ones that use L_2 -Delaunay

⁸The *lightness* of a geometric graph G on a pointset P is defined as ratio of the weight of G to that of a Euclidean minimum spanning tree on P .

triangulations, BGS05 is the slowest due to the overhead of creation of temporary geometric graphs needed to control the degree and stretch-factor of the output spanners. Refer to Section 2 to see more details on this algorithm. The fastest algorithms are KPX10, BSX09, LW04, and KX12. The main reason behind their speedy performance is fast construction of L_2 -Delaunay triangulations and lightweight processing of the triangulations for spanner construction. The BHS18, BCC12-7, and BCC12-6 algorithms came out quite close to the above four algorithms. Note that these three algorithms also use L_2 -Delaunay triangulation as the starting point. The same observations hold for the real-world pointsets used in our experiments. See the table presented in Fig. 9 for the runtimes in seconds.

2. *Degree.* Refer to Fig. 7. In the tables, Δ denotes the theoretical degree upper bound, as claimed by the authors of these algorithms, $\max \Delta_{\text{observed}}$ denotes the maximum degree observed in our experiments, $\text{avg } \Delta_{\text{observed}}$ denotes the observed average degree, and $\text{avg } \Delta_{\text{vertex}}$ denotes the observed average degree per vertex. In our experiments, we find that spanners generated by BGS05, LW04, and BSX09 have degrees much less than the degree upper-bounds derived by the authors. While it cannot be denied that there could be special examples where these upper-bounds are actually achieved, the maximum degrees achieved in our experiments are 14, 11, and 9, respectively. Note that the theoretical degree upper bounds are 27, 23, and 17, respectively. For the remaining eight algorithms, the claimed degree upper-bounds are achieved in our experiments thereby showing the analyses obtained by the authors of those algorithms are tight. However, the degree bound claimed by the authors of BCC12-6 appears incorrect. We present an example in the Appendix (Section 6.2) where the degree of the spanner generated by this algorithm exceeds 6 (in fact, it is 7 in this example). For every algorithm, we find that the average degree of the generated spanners is not far away from the maximum observed degrees. It shows that the algorithms are consistent in constructing the spanners. The average degree per vertex is another way to judge the quality of the spanners. In this regard, we find that it is always between 6 and 3 everywhere and is quite reasonable for practical purposes. This shows that all these algorithms are very careful when it comes to the selection of spanner edges. The lowest values are achieved by BKPX15 and KPT17. For the real-world pointsets, we find similar performance from the algorithms when it comes to the degree and degree per vertex of the spanners. This is quite surprising since these real-world pointsets do not follow specific distributions. Refer to Figs. 10 and 11 for more details. Note that BGS05 has produced a degree-15 spanner for the `vlsi` pointset. In contrast, for the synthetic pointsets the highest degree we could observe is 14.
3. *Stretch factor.* Refer to Fig. 8. In the tables, t denotes the theoretical stretch factor, as derived by the authors of these algorithms; t_{max} denotes the maximum stretch factor observed in our experiments, and t_{avg} denotes the average observed stretch factor. Among the eleven algorithms, KPX10 has the lowest guaranteed stretch factor - it is 2.9. The stretch factors of the spanners generated by KPX10 are always less than 1.6, thereby making it the best among the eleven algorithms in terms of stretch factor. In this regard, BKPX15 turned out to be the worst; the largest stretch factor we have observed is 7.242, although it is substantially less than the theoretical stretch factor upper bound of 156.8. Its competitor KPX17 that can also generate degree-4 plane spanners has a lower observed maximum stretch factor - it is 5.236 (theoretical upper bound is 20 for this algorithm). Overall, we find that the stretch factors of the generated spanners are much less than the claimed theoretical upper bounds. This shows that the generated spanners are well-constructed in practice. With the exception of BKPX15, we find that the average stretch factors are quite close to the maximum stretch factors. Now let us turn our attention to the real-world pointsets. Refer to Fig. 12. Once again KPX10 produced lowest stretch factor spanners. The stretch factors seem quite reasonable everywhere except the two cases of `vlsi` and `uber` pointsets when fed to BKPX15. The produced spanners have stretch factors of 11.535 and 27.929, respectively. The latter is interesting since the lower bound example constructed by the authors in [11] for the worst-case stretch factor of the spanners produced by BKPX15 has a stretch factor of $7 + 7\sqrt{2} \approx 16.899$. The `uber` pointset beats this lower bound.
4. *Lightness.* Since a minimum spanning tree is the cheapest (in terms of the sum of the total length of the edges) way to connect n points, lightness can be used to judge the quality of spanners. This metric

is beneficial when spanners are used for constructing computer or transportation networks. Refer to Fig. 8. Lightness is denoted by ℓ . With a few exceptions, we find that lightness somewhat correlates with degree. This is because using a lower number of carefully placed spanner edges usually leads to lower lightness. The spanners generated by BGS05 are always found to have the highest lightness. This is expected because of their high degrees. Although, the difference in degree of the spanners generated by BGXS05 and LW04 is marginal (around 2), the difference between their lightness is substantial (approximately 6 for some cases). On the other hand, the degree-4 spanners generated by KPT17 have the lowest lightnesses (less than 2.9 everywhere). Interestingly, although BKPX15 generates degree-4 spanners, their lightness is found to be approximately twice that of the ones generated by KPT17. In fact, their lightness turned out to be one of the highest. This shows that KPT17 is more careful when it comes to placing long edges. The lightnesses of the spanners generated for real-world pointsets follow a similar trend, and we did not observe anything special. Refer to Fig. 13 for more details.

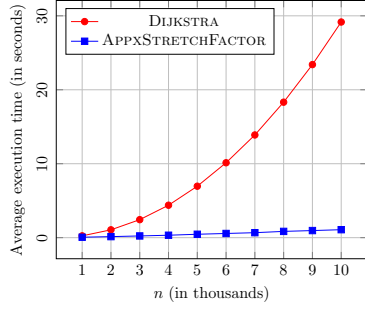
Remark. In our experiments, we find that the spanners' degree, stretch factor, and lightness remained somewhat constant with the increase in n . Hence, we do not present plots for them.

5 Conclusions

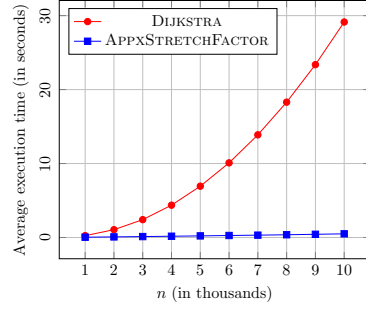
Since there are various ways (speed, degree, stretch factor, lightness) to judge the eleven algorithms, it is hard to declare the winner(s). So, based on our experimental observations, we come to the following conclusions (are our recommendations as well):

- If speedy performance is the main concern, we recommend using KPX10, BSX09, LW04, or KX12.
- When it comes to minimization of degree, we recommend using BCC12-7 or BHS18 since they produce spanners of reasonable degrees in practice. If degree-4 spanners are desired, we recommend using BKPX15 since KPT17 is much slower in practice.
- In terms of stretch factor, we find the KPX10 as the clear winner. This is particularly important in the study of geometric spanners since not much is known about fast construction of low stretch factor spanners ($t \approx 1.6$) in the plane having at most $3n$ edges. However, the spanners produced by it have higher degrees compared to the ones produced by some of the other algorithms such as BCC12 and BHS18.
- In our experiments, KPT17 produced spanners with the lowest lightnesses. But in practice, we found it to be very slow compared to the other algorithms except for BGHP10 (which is as slow as KPT17). If degree-4 spanners is not a requirement, we recommend using BHS18 or BCC12-7 since they produced spanners of reasonable lightness (less than 4 most of the times).

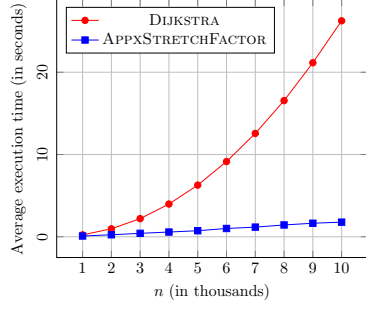
Acknowledgment. We sincerely thank Nicolas Bonichon (one of the authors of BKPX15) for sharing the applet code for the algorithm BKPX15 [11]. The code has helped us to understand the algorithm clearly and create a CGAL implementation of the algorithm.



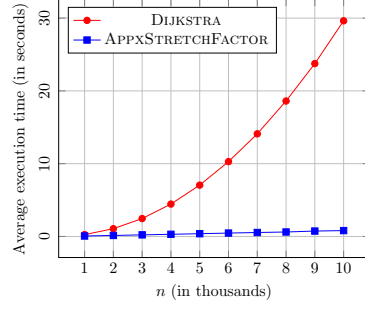
(a) uni-square



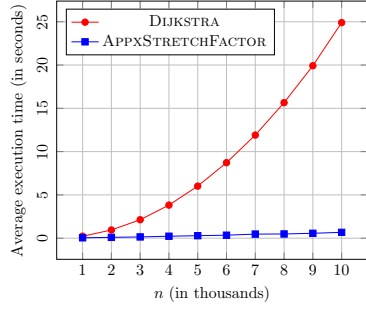
(b) uni-disk



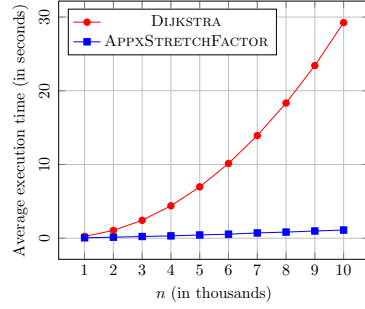
(c) normal-clustered



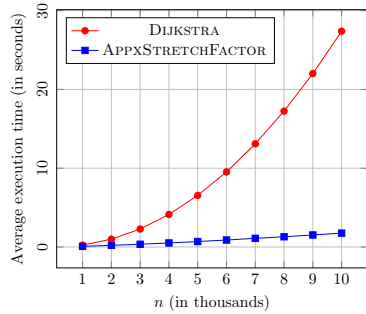
(d) normal



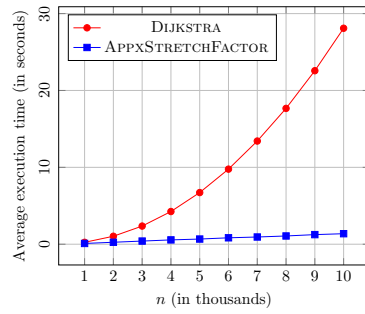
(e) grid-contiguous



(f) grid-random



(g) annulus



(h) galaxy

Figure 5: Runtime comparison: Dijkstra (run from every vertex) vs APPXSTRETCHFACTOR. For every value of n , we have used $11 \cdot 5 = 55$ spanner samples since there are 11 algorithms and 5 pointsets were generated for that value of n using the same distribution.

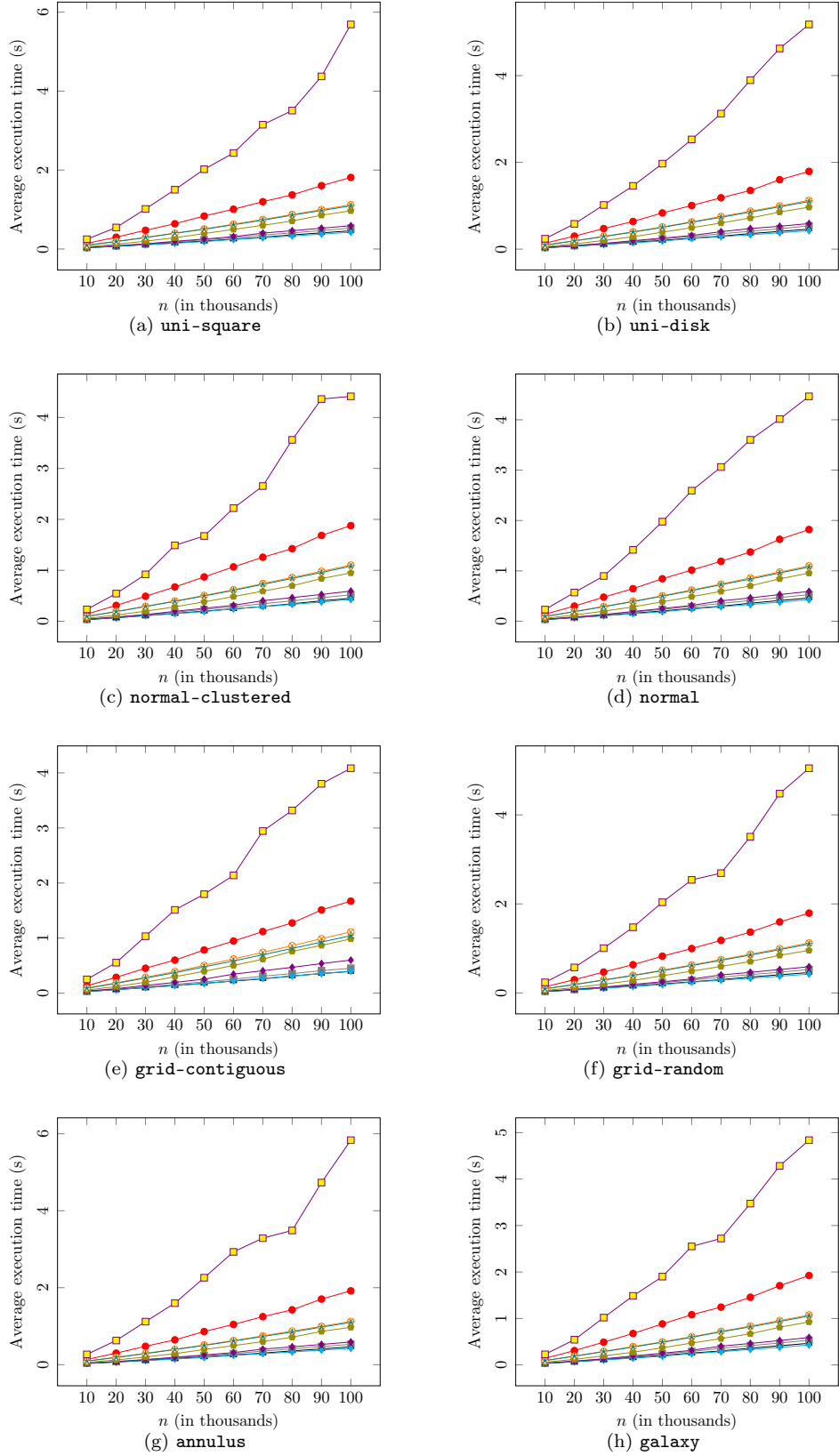


Figure 6: Runtime comparisons of the nine algorithms (BGHP10 and KPT17 are excluded).

| Algorithm | Δ | max Δ_{observed} | avg Δ_{observed} | avg Δ_{vertex} |
|-----------|----------|--------------------------------|--------------------------------|------------------------------|
| BGS05 | 27 | 13 | 11.580 | 5.745 |
| LW04 | 23 | 11 | 9.820 | 5.148 |
| BSX09 | 17 | 9 | 7.840 | 4.392 |
| KPX10 | 14 | 14 | 12.980 | 5.994 |
| KX12 | 11 | 10 | 9.960 | 5.449 |
| BHS18 | 8 | 7 | 6.980 | 4.113 |
| BCC12-7 | 7 | 7 | 7.000 | 4.337 |
| BCC12-6 | 6 | 7 | 6.820 | 4.016 |
| BGHP10 | 6 | 6 | 6.000 | 4.240 |
| BKPX15 | 4 | 4 | 4.000 | 3.328 |
| KPT17 | 4 | 4 | 4.000 | 3.140 |

(a) uni-square

| Algorithm | Δ | max Δ_{observed} | avg Δ_{observed} | avg Δ_{vertex} |
|-----------|----------|--------------------------------|--------------------------------|------------------------------|
| BGS05 | 27 | 12 | 11.540 | 5.744 |
| LW04 | 23 | 11 | 9.880 | 5.146 |
| BSX09 | 17 | 9 | 7.760 | 4.389 |
| KPX10 | 14 | 13 | 12.420 | 5.993 |
| KX12 | 11 | 10 | 9.980 | 5.451 |
| BHS18 | 8 | 7 | 6.200 | 4.109 |
| BCC12-7 | 7 | 7 | 7.000 | 4.335 |
| BCC12-6 | 6 | 7 | 6.020 | 4.012 |
| BGHP10 | 6 | 6 | 6.000 | 4.239 |
| BKPX15 | 4 | 4 | 4.000 | 3.319 |
| KPT17 | 4 | 4 | 4.000 | 3.141 |

(b) uni-disk

| Algorithm | Δ | max Δ_{observed} | avg Δ_{observed} | avg Δ_{vertex} |
|-----------|----------|--------------------------------|--------------------------------|------------------------------|
| BGS05 | 27 | 13 | 11.600 | 5.750 |
| LW04 | 23 | 11 | 9.800 | 5.154 |
| BSX09 | 17 | 9 | 7.860 | 4.392 |
| KPX10 | 14 | 14 | 12.820 | 5.996 |
| KX12 | 11 | 10 | 9.980 | 5.450 |
| BHS18 | 8 | 7 | 6.100 | 4.110 |
| BCC12-7 | 7 | 7 | 7.000 | 4.334 |
| BCC12-6 | 6 | 6 | 6.000 | 4.010 |
| BGHP10 | 6 | 6 | 6.000 | 4.245 |
| BKPX15 | 4 | 4 | 4.000 | 3.327 |
| KPT17 | 4 | 4 | 4.000 | 3.144 |

(c) normal-clustered

| Algorithm | Δ | max Δ_{observed} | avg Δ_{observed} | avg Δ_{vertex} |
|-----------|----------|--------------------------------|--------------------------------|------------------------------|
| BGS05 | 27 | 13 | 11.740 | 5.751 |
| LW04 | 23 | 11 | 9.760 | 5.158 |
| BSX09 | 17 | 9 | 7.880 | 4.395 |
| KPX10 | 14 | 14 | 12.320 | 5.997 |
| KX12 | 11 | 10 | 9.940 | 5.452 |
| BHS18 | 8 | 7 | 6.060 | 4.117 |
| BCC12-7 | 7 | 7 | 7.000 | 4.346 |
| BCC12-6 | 6 | 6 | 6.000 | 4.023 |
| BGHP10 | 6 | 6 | 6.000 | 4.254 |
| BKPX15 | 4 | 4 | 4.000 | 3.327 |
| KPT17 | 4 | 4 | 4.000 | 3.150 |

(d) normal

| Algorithm | Δ | max Δ_{observed} | avg Δ_{observed} | avg Δ_{vertex} |
|-----------|----------|--------------------------------|--------------------------------|------------------------------|
| BGS05 | 27 | 11 | 11.000 | 5.919 |
| LW04 | 23 | 9 | 7.920 | 5.099 |
| BSX09 | 17 | 9 | 7.660 | 4.412 |
| KPX10 | 14 | 12 | 11.880 | 5.993 |
| KX12 | 11 | 11 | 10.000 | 5.987 |
| BHS18 | 8 | 7 | 7.000 | 4.825 |
| BCC12-7 | 7 | 7 | 7.000 | 5.160 |
| BCC12-6 | 6 | 7 | 6.960 | 4.361 |
| BGHP10 | 6 | 6 | 6.000 | 4.979 |
| BKPX15 | 4 | 4 | 4.000 | 3.350 |
| KPT17 | 4 | 4 | 4.000 | 3.537 |

(e) grid-contiguous

| Algorithm | Δ | max Δ_{observed} | avg Δ_{observed} | avg Δ_{vertex} |
|-----------|----------|--------------------------------|--------------------------------|------------------------------|
| BGS05 | 27 | 13 | 11.540 | 5.745 |
| LW04 | 23 | 11 | 9.900 | 5.148 |
| BSX09 | 17 | 9 | 7.980 | 4.391 |
| KPX10 | 14 | 14 | 12.940 | 5.995 |
| KX12 | 11 | 10 | 9.980 | 5.449 |
| BHS18 | 8 | 7 | 6.960 | 4.114 |
| BCC12-7 | 7 | 7 | 7.000 | 4.338 |
| BCC12-6 | 6 | 7 | 6.740 | 4.016 |
| BGHP10 | 6 | 6 | 6.000 | 4.240 |
| BKPX15 | 4 | 4 | 4.000 | 3.327 |
| KPT17 | 4 | 4 | 4.000 | 3.140 |

(f) grid-random

| Algorithm | Δ | max Δ_{observed} | avg Δ_{observed} | avg Δ_{vertex} |
|-----------|----------|--------------------------------|--------------------------------|------------------------------|
| BGS05 | 27 | 13 | 11.520 | 5.730 |
| LW04 | 23 | 11 | 9.740 | 5.130 |
| BSX09 | 17 | 9 | 8.100 | 4.382 |
| KPX10 | 14 | 14 | 13.180 | 5.987 |
| KX12 | 11 | 11 | 10.300 | 5.448 |
| BHS18 | 8 | 7 | 6.960 | 4.098 |
| BCC12-7 | 7 | 7 | 7.000 | 4.313 |
| BCC12-6 | 6 | 8 | 6.940 | 3.994 |
| BGHP10 | 6 | 6 | 6.000 | 4.230 |
| BKPX15 | 4 | 4 | 4.000 | 3.315 |
| KPT17 | 4 | 4 | 4.000 | 3.130 |

(g) annulus

| Algorithm | Δ | max Δ_{observed} | avg Δ_{observed} | avg Δ_{vertex} |
|-----------|----------|--------------------------------|--------------------------------|------------------------------|
| BGS05 | 27 | 14 | 12.320 | 5.736 |
| LW04 | 23 | 11 | 9.920 | 5.134 |
| BSX09 | 17 | 9 | 8.180 | 4.384 |
| KPX10 | 14 | 14 | 13.680 | 5.993 |
| KX12 | 11 | 11 | 10.000 | 5.434 |
| BHS18 | 8 | 7 | 6.580 | 4.090 |
| BCC12-7 | 7 | 7 | 7.000 | 4.290 |
| BCC12-6 | 6 | 7 | 6.120 | 3.970 |
| BGHP10 | 6 | 6 | 6.000 | 4.228 |
| BKPX15 | 4 | 4 | 4.000 | 3.326 |
| KPT17 | 4 | 4 | 4.000 | 3.131 |

(h) galaxy

Figure 7: Degree comparisons of the spanners generated by the eleven algorithms.

| Algorithm | t | t_{\max} | t_{avg} | Algorithm | ℓ |
|-----------|-------|------------|------------------|-----------|--------|
| BGS05 | 8.3 | 2.687 | 2.215 | BGS05 | 10.209 |
| LW04 | 6.4 | 2.687 | 2.349 | LW04 | 4.366 |
| BSX09 | 23.6 | 4.284 | 3.666 | BSX09 | 3.585 |
| KPX10 | 2.9 | 1.519 | 1.453 | KPX10 | 5.378 |
| KX12 | 5.7 | 2.021 | 1.848 | KX12 | 4.728 |
| BHS18 | 4.4 | 2.812 | 2.548 | BHS18 | 3.315 |
| BCC12-7 | 11.6 | 2.433 | 2.152 | BCC12-7 | 3.636 |
| BCC12-6 | 81.7 | 2.894 | 2.494 | BCC12-6 | 3.298 |
| BGHP10 | 6 | 3.204 | 2.755 | BGHP10 | 3.429 |
| BKPX15 | 156.8 | 4.692 | 3.505 | BKPX15 | 4.824 |
| KPT17 | 20 | 4.895 | 4.067 | KPT17 | 2.261 |

(a) uni-square

| Algorithm | t | t_{\max} | t_{avg} | Algorithm | ℓ |
|-----------|-------|------------|------------------|-----------|--------|
| BGS05 | 8.3 | 2.409 | 2.202 | BGS05 | 10.014 |
| LW04 | 6.4 | 2.525 | 2.325 | LW04 | 4.310 |
| BSX09 | 23.6 | 4.267 | 3.656 | BSX09 | 3.528 |
| KPX10 | 2.9 | 1.497 | 1.450 | KPX10 | 5.279 |
| KX12 | 5.7 | 2.034 | 1.857 | KX12 | 4.661 |
| BHS18 | 4.4 | 3.152 | 2.587 | BHS18 | 3.275 |
| BCC12-7 | 11.6 | 2.460 | 2.167 | BCC12-7 | 3.597 |
| BCC12-6 | 81.7 | 2.998 | 2.460 | BCC12-6 | 3.261 |
| BGHP10 | 6 | 3.034 | 2.782 | BGHP10 | 3.415 |
| BKPX15 | 156.8 | 4.255 | 3.501 | BKPX15 | 4.702 |
| KPT17 | 20 | 5.050 | 4.052 | KPT17 | 2.259 |

(b) uni-disk

| Algorithm | t | t_{\max} | t_{avg} | Algorithm | ℓ |
|-----------|-------|------------|------------------|-----------|--------|
| BGS05 | 8.3 | 2.555 | 2.214 | BGS05 | 12.802 |
| LW04 | 6.4 | 2.522 | 2.327 | LW04 | 5.220 |
| BSX09 | 23.6 | 4.226 | 3.664 | BSX09 | 4.345 |
| KPX10 | 2.9 | 1.489 | 1.448 | KPX10 | 6.752 |
| KX12 | 5.7 | 2.126 | 1.856 | KX12 | 5.611 |
| BHS18 | 4.4 | 3.098 | 2.571 | BHS18 | 3.726 |
| BCC12-7 | 11.6 | 2.457 | 2.161 | BCC12-7 | 4.031 |
| BCC12-6 | 81.7 | 2.814 | 2.476 | BCC12-6 | 3.680 |
| BGHP10 | 6 | 3.400 | 2.804 | BGHP10 | 3.870 |
| BKPX15 | 156.8 | 3.967 | 3.500 | BKPX15 | 5.328 |
| KPT17 | 20 | 4.852 | 4.032 | KPT17 | 2.545 |

(c) normal-clustered

| Algorithm | t | t_{\max} | t_{avg} | Algorithm | ℓ |
|-----------|-------|------------|------------------|-----------|--------|
| BGS05 | 8.3 | 2.504 | 2.198 | BGS05 | 10.111 |
| LW04 | 6.4 | 2.575 | 2.329 | LW04 | 4.345 |
| BSX09 | 23.6 | 4.172 | 3.701 | BSX09 | 3.553 |
| KPX10 | 2.9 | 1.500 | 1.450 | KPX10 | 5.319 |
| KX12 | 5.7 | 2.493 | 1.872 | KX12 | 4.702 |
| BHS18 | 4.4 | 3.090 | 2.538 | BHS18 | 3.288 |
| BCC12-7 | 11.6 | 2.438 | 2.173 | BCC12-7 | 3.603 |
| BCC12-6 | 81.7 | 2.737 | 2.447 | BCC12-6 | 3.264 |
| BGHP10 | 6 | 3.178 | 2.731 | BGHP10 | 3.431 |
| BKPX15 | 156.8 | 4.344 | 3.507 | BKPX15 | 4.748 |
| KPT17 | 20 | 5.236 | 3.990 | KPT17 | 2.267 |

(d) normal

| Algorithm | t | t_{\max} | t_{avg} | Algorithm | ℓ |
|-----------|-------|------------|------------------|-----------|--------|
| BGS05 | 8.3 | 3.000 | 2.812 | BGS05 | 6.911 |
| LW04 | 6.4 | 3.000 | 2.965 | LW04 | 2.820 |
| BSX09 | 23.6 | 3.000 | 3.000 | BSX09 | 2.455 |
| KPX10 | 2.9 | 1.414 | 1.414 | KPX10 | 3.506 |
| KX12 | 5.7 | 1.414 | 1.414 | KX12 | 3.480 |
| BHS18 | 4.4 | 1.414 | 1.414 | BHS18 | 2.613 |
| BCC12-7 | 11.6 | 1.414 | 1.414 | BCC12-7 | 2.850 |
| BCC12-6 | 81.7 | 1.414 | 1.414 | BCC12-6 | 2.286 |
| BGHP10 | 6 | 1.414 | 1.414 | BGHP10 | 2.705 |
| BKPX15 | 156.8 | 7.242 | 6.337 | BKPX15 | 3.852 |
| KPT17 | 20 | 3.000 | 3.000 | KPT17 | 1.915 |

(e) grid-contiguous

| Algorithm | t | t_{\max} | t_{avg} | Algorithm | ℓ |
|-----------|-------|------------|------------------|-----------|--------|
| BGS05 | 8.3 | 2.413 | 2.199 | BGS05 | 10.213 |
| LW04 | 6.4 | 2.707 | 2.364 | LW04 | 4.367 |
| BSX09 | 23.6 | 4.080 | 3.686 | BSX09 | 3.585 |
| KPX10 | 2.9 | 1.508 | 1.452 | KPX10 | 5.382 |
| KX12 | 5.7 | 2.153 | 1.838 | KX12 | 4.730 |
| BHS18 | 4.4 | 2.905 | 2.555 | BHS18 | 3.318 |
| BCC12-7 | 11.6 | 2.349 | 2.126 | BCC12-7 | 3.637 |
| BCC12-6 | 81.7 | 2.698 | 2.441 | BCC12-6 | 3.300 |
| BGHP10 | 6 | 3.171 | 2.807 | BGHP10 | 3.431 |
| BKPX15 | 156.8 | 4.056 | 3.496 | BKPX15 | 4.825 |
| KPT17 | 20 | 4.777 | 4.036 | KPT17 | 2.261 |

(f) grid-random

| Algorithm | t | t_{\max} | t_{avg} | Algorithm | ℓ |
|-----------|-------|------------|------------------|-----------|--------|
| BGS05 | 8.3 | 2.490 | 2.185 | BGS05 | 10.375 |
| LW04 | 6.4 | 2.735 | 2.344 | LW04 | 4.445 |
| BSX09 | 23.6 | 4.294 | 3.668 | BSX09 | 3.675 |
| KPX10 | 2.9 | 1.557 | 1.522 | KPX10 | 5.524 |
| KX12 | 5.7 | 2.078 | 1.862 | KX12 | 4.833 |
| BHS18 | 4.4 | 3.286 | 2.559 | BHS18 | 3.351 |
| BCC12-7 | 11.6 | 2.574 | 2.162 | BCC12-7 | 3.661 |
| BCC12-6 | 81.7 | 2.922 | 2.466 | BCC12-6 | 3.321 |
| BGHP10 | 6 | 3.077 | 2.756 | BGHP10 | 6.154 |
| BKPX15 | 156.8 | 4.226 | 3.527 | BKPX15 | 7.273 |
| KPT17 | 20 | 4.637 | 4.002 | KPT17 | 3.544 |

(g) annulus

| Algorithm | t | t_{\max} | t_{avg} | Algorithm | ℓ |
|-----------|-------|------------|------------------|-----------|--------|
| BGS05 | 8.3 | 2.452 | 2.209 | BGS05 | 12.119 |
| LW04 | 6.4 | 2.673 | 2.323 | LW04 | 5.114 |
| BSX09 | 23.6 | 4.077 | 3.716 | BSX09 | 4.250 |
| KPX10 | 2.9 | 1.512 | 1.451 | KPX10 | 6.521 |
| KX12 | 5.7 | 2.552 | 1.878 | KX12 | 5.326 |
| BHS18 | 4.4 | 3.147 | 2.587 | BHS18 | 3.686 |
| BCC12-7 | 11.6 | 2.352 | 2.149 | BCC12-7 | 3.949 |
| BCC12-6 | 81.7 | 2.803 | 2.483 | BCC12-6 | 3.608 |
| BGHP10 | 6 | 3.309 | 2.773 | BGHP10 | 4.398 |
| BKPX15 | 156.8 | 6.833 | 3.615 | BKPX15 | 5.806 |
| KPT17 | 20 | 4.867 | 4.049 | KPT17 | 2.871 |

(h) galaxy

Figure 8: Stretch-factor and lightness comparisons of the spanners generated by the eleven algorithms.

| Pointset | n | BGS05 | LW04 | BSX09 | KPX10 | KX12 | BHS18 | BCC12-7 | BCC12-6 | BGHP10 | BKPX15 | KPT17 |
|-----------|---------|---------|--------|--------|--------|--------|---------|---------|---------|---------|----------|---------|
| burma | 33708 | 2.888 | 0.711 | 0.627 | 0.599 | 0.832 | 1.101 | 1.569 | 1.549 | 173.528 | 5.885 | 173.447 |
| birch3 | 99801 | 9.700 | 2.459 | 2.139 | 2.117 | 3.001 | 4.458 | 5.188 | 5.079 | 640.619 | 20.003 | 641.839 |
| mona-lisa | 100000 | 8.527 | 2.450 | 2.127 | 2.236 | 3.189 | 4.960 | 5.863 | 5.588 | 704.980 | 27.988 | 706.000 |
| KDDCU2D | 104297 | 10.024 | 2.579 | 2.252 | 2.250 | 3.146 | 4.837 | 5.569 | 5.460 | 811.921 | 21.424 | 812.665 |
| usa | 115475 | 10.575 | 2.878 | 2.497 | 2.521 | 3.559 | 5.600 | 6.426 | 6.258 | 1033.99 | 35.769 | 1035.64 |
| europa | 168896 | 15.516 | 4.520 | 3.985 | 3.968 | 5.685 | 8.386 | 9.402 | 9.230 | 1494.69 | 39.133 | 1497.09 |
| wiki | 317695 | 35.374 | 9.041 | 7.687 | 8.004 | 11.432 | 17.274 | 18.105 | 17.794 | 3507.06 | 98.975 | 3510.20 |
| vsli | 744710 | 81.461 | 21.655 | 19.457 | 19.693 | 28.165 | 46.630 | 47.297 | 46.183 | 13296.6 | 509.795 | 13312.2 |
| china | 808693 | 91.243 | 24.078 | 21.642 | 21.775 | 30.793 | 52.637 | 54.367 | 53.029 | 17028.4 | 451.383 | 17057.3 |
| uber | 1381253 | 170.493 | 42.199 | 38.227 | 38.268 | 54.486 | 89.577 | 94.444 | 92.359 | 29584.6 | 1689.042 | 29633.1 |
| world | 1904711 | 259.147 | 57.657 | 52.078 | 52.337 | 74.570 | 125.078 | 128.316 | 125.787 | 58707.7 | 1358.70 | 58780.3 |

Figure 9: Average execution time (in seconds).

| Pointset | n | BGS05 | LW04 | BSX09 | KPX10 | KX12 | BHS18 | BCC12-7 | BCC12-6 | BGHP10 | BKPX15 | KPT17 |
|-----------|---------|-------|------|-------|-------|------|-------|---------|---------|--------|--------|-------|
| burma | 33708 | 11 | 10 | 8 | 14 | 11 | 6 | 7 | 6 | 6 | 4 | 4 |
| birch3 | 99801 | 13 | 10 | 8 | 13 | 11 | 6 | 7 | 6 | 6 | 4 | 4 |
| mona-lisa | 100000 | 11 | 8 | 8 | 12 | 10 | 7 | 7 | 7 | 6 | 4 | 4 |
| KDDCU2D | 104297 | 13 | 10 | 8 | 14 | 10 | 6 | 7 | 7 | 6 | 4 | 4 |
| usa | 115475 | 12 | 10 | 8 | 14 | 11 | 7 | 7 | 7 | 6 | 4 | 4 |
| europa | 168896 | 12 | 10 | 8 | 13 | 10 | 6 | 7 | 6 | 6 | 4 | 4 |
| wiki | 317695 | 14 | 10 | 9 | 14 | 11 | 7 | 7 | 7 | 6 | 4 | 4 |
| vsli | 744710 | 15 | 11 | 9 | 14 | 10 | 7 | 7 | 7 | 6 | 4 | 4 |
| china | 808693 | 13 | 11 | 9 | 14 | 11 | 7 | 7 | 6 | 6 | 4 | 4 |
| uber | 1381253 | 13 | 11 | 9 | 14 | 10 | 7 | 7 | 6 | 6 | 4 | 4 |
| world | 1904711 | 14 | 11 | 9 | 14 | 11 | 7 | 7 | 7 | 6 | 4 | 4 |

Figure 10: Degree of the spanners.

| Pointset | n | BGS05 | LW04 | BSX09 | KPX10 | KX12 | BHS18 | BCC12-7 | BCC12-6 | BGHP10 | BKPX15 | KPT17 |
|-----------|---------|-------|-------|-------|-------|-------|-------|---------|---------|--------|--------|-------|
| burma | 33708 | 5.761 | 5.192 | 4.454 | 5.994 | 5.512 | 4.166 | 4.292 | 4.068 | 4.347 | 3.346 | 3.187 |
| birch3 | 99801 | 5.745 | 5.149 | 4.417 | 5.995 | 5.429 | 4.081 | 4.287 | 3.970 | 4.222 | 3.327 | 3.130 |
| mona-lisa | 100000 | 5.938 | 5.596 | 4.617 | 5.996 | 5.981 | 5.259 | 5.741 | 5.165 | 5.434 | 3.572 | 3.613 |
| KDDCU2D | 104297 | 5.720 | 5.127 | 4.399 | 5.985 | 5.390 | 4.047 | 4.294 | 4.015 | 4.216 | 3.325 | 3.122 |
| usa | 115475 | 5.761 | 5.208 | 4.447 | 5.993 | 5.529 | 4.248 | 4.493 | 4.132 | 4.398 | 3.366 | 3.211 |
| europa | 168896 | 5.745 | 5.160 | 4.427 | 5.997 | 5.438 | 4.090 | 4.310 | 3.991 | 4.234 | 3.325 | 3.135 |
| wiki | 317695 | 5.679 | 5.061 | 4.379 | 5.987 | 5.333 | 3.931 | 4.016 | 3.732 | 4.070 | 3.308 | 3.016 |
| vsli | 744710 | 5.749 | 5.152 | 4.416 | 5.994 | 5.438 | 4.096 | 4.334 | 4.007 | 4.277 | 3.316 | 3.176 |
| china | 808693 | 5.770 | 5.209 | 4.437 | 5.996 | 5.519 | 4.245 | 4.506 | 4.154 | 4.368 | 3.344 | 3.208 |
| uber | 1381253 | 5.742 | 5.147 | 4.394 | 5.996 | 5.437 | 4.086 | 4.288 | 3.968 | 4.232 | 3.326 | 3.130 |
| world | 1904711 | 5.748 | 5.171 | 4.438 | 5.991 | 5.489 | 4.151 | 4.371 | 4.020 | 4.318 | 3.344 | 3.168 |

Figure 11: Average degree per vertex.

| Pointset | n | BGS05 | LW04 | BSX09 | KPX10 | KX12 | BHS18 | BCC12-7 | BCC12-6 | BGHP10 | BKPX15 | KPT17 |
|-----------|---------|-------|-------|-------|-------|-------|-------|---------|---------|--------|--------|-------|
| burma | 33708 | 2.414 | 2.414 | 3.681 | 1.482 | 1.738 | 2.856 | 2.156 | 2.162 | 3.161 | 4.404 | 4.409 |
| birch3 | 99801 | 2.233 | 2.234 | 3.520 | 1.481 | 1.923 | 2.719 | 2.318 | 2.460 | 2.933 | 3.624 | 4.102 |
| mona-lisa | 100000 | 2.523 | 2.237 | 3.373 | 1.413 | 1.609 | 2.872 | 1.778 | 2.278 | 2.872 | 4.190 | 3.768 |
| KDDCU2D | 104297 | 2.211 | 2.435 | 3.953 | 1.492 | 2.068 | 2.937 | 2.174 | 2.603 | 2.937 | 4.299 | 4.218 |
| usa | 115475 | 2.300 | 2.351 | 3.564 | 1.480 | 2.038 | 2.765 | 2.241 | 2.576 | 3.430 | 3.740 | 4.455 |
| europa | 168896 | 2.245 | 2.343 | 4.072 | 1.459 | 1.840 | 2.745 | 2.310 | 2.659 | 2.981 | 4.081 | 4.121 |
| wiki | 317695 | 2.408 | 2.421 | 3.926 | 1.458 | 1.978 | 2.757 | 2.350 | 2.610 | 3.222 | 4.353 | 4.017 |
| vsli | 744710 | 2.468 | 2.999 | 3.650 | 1.471 | 1.970 | 2.942 | 2.355 | 2.263 | 3.521 | 11.535 | 5.472 |
| china | 808693 | 2.478 | 2.421 | 4.082 | 1.511 | 2.055 | 2.731 | 2.237 | 2.711 | 2.981 | 4.061 | 4.506 |
| uber | 1381253 | 2.535 | 2.418 | 3.987 | 1.485 | 2.204 | 2.902 | 2.407 | 2.816 | 3.073 | 27.929 | 4.966 |
| world | 1904711 | 2.989 | 2.961 | 4.228 | 1.522 | 1.997 | 3.056 | 2.357 | 2.657 | 3.545 | 6.140 | 5.422 |

Figure 12: Stretch factor of the spanners.

| Pointset | n | BGS05 | LW04 | BSX09 | KPX10 | KX12 | BHS18 | BCC12-7 | BCC12-6 | BGHP10 | BKPX15 | KPT17 |
|-----------|---------|--------|-------|-------|-------|-------|-------|---------|---------|--------|--------|-------|
| burma | 33708 | 10.755 | 4.538 | 3.768 | 5.672 | 4.922 | 3.374 | 3.609 | 3.365 | 3.620 | 5.048 | 2.345 |
| birch3 | 99801 | 11.008 | 4.660 | 3.845 | 5.805 | 4.989 | 3.453 | 3.770 | 3.434 | 3.699 | 5.124 | 2.426 |
| mona-lisa | 100000 | 7.070 | 3.259 | 2.656 | 3.574 | 3.542 | 3.012 | 3.326 | 2.934 | 3.147 | 3.934 | 1.994 |
| KDDCU2D | 104297 | 10.576 | 4.491 | 3.719 | 5.605 | 4.830 | 3.316 | 3.670 | 3.355 | 3.511 | 4.954 | 2.311 |
| usa | 115475 | 10.264 | 4.427 | 3.663 | 5.431 | 4.753 | 3.336 | 3.642 | 3.305 | 3.602 | 4.935 | 2.336 |
| europa | 168896 | 10.136 | 4.365 | 3.593 | 5.395 | 4.736 | 3.274 | 3.588 | 3.233 | 3.428 | 4.746 | 2.254 |
| wiki | 317695 | 12.137 | 5.087 | 4.227 | 6.555 | 5.385 | 3.607 | 3.877 | 3.525 | 3.860 | 5.477 | 2.481 |
| vsli | 744710 | 11.344 | 4.850 | 4.024 | 5.989 | 5.110 | 3.521 | 3.899 | 3.539 | 3.864 | 5.130 | 2.513 |
| china | 808693 | 9.918 | 4.304 | 3.531 | 5.232 | 4.605 | 3.286 | 3.594 | 3.247 | 3.445 | 4.719 | 2.263 |
| uber | 1381253 | 11.225 | 4.497 | 4.291 | 5.900 | 5.424 | 2.797 | 2.843 | 2.888 | 3.015 | 4.584 | 1.861 |
| world | 1904711 | 11.145 | 4.744 | 3.923 | 5.917 | 5.003 | 3.476 | 3.777 | 3.432 | 3.967 | 5.272 | 2.541 |

Figure 13: Lightness of the spanners.

References

- [1] www.math.uwaterloo.ca/tsp/.
- [2] Pankaj K Agarwal, Rolf Klein, Christian Knauer, Stefan Langerman, Pat Morin, Micha Sharir, and Michael Soss. Computing the detour and spanning ratio of paths, trees, and cycles in 2d and 3d. *Discrete & Computational Geometry*, 39(1):17–37, 2008.
- [3] Fred Anderson, Anirban Ghosh, Matthew Graham, Lucas Mougeot, and David Wisnosky. An interactive tool for experimenting with bounded-degree plane geometric spanners (media exposition). In *37th International Symposium on Computational Geometry (SoCG 2021)*. Schloss Dagstuhl-Leibniz-Zentrum für Informatik, 2021.
- [4] Davood Bakhshesh and Mohammad Farshi. A degree 3 plane 5.19-spanner for points in convex position. In *CCCG*, pages 226–232, 2020.
- [5] Jon Louis Bentley. K-d trees for semidynamic point sets. In *Proceedings of the Sixth Annual Symposium on Computational Geometry*, pages 187–197, 1990.
- [6] Ahmad Biniiaz. Plane hop spanners for unit disk graphs: Simpler and better. *Comput. Geom.*, 89:101622, 2020.
- [7] Ahmad Biniiaz, Prosenjit Bose, Jean-Lou De Carufel, Cyril Gavoille, Anil Maheshwari, and Michiel Smid. Towards plane spanners of degree 3. *Journal of Computational Geometry*, 8(1):11–31, 2017.
- [8] Nicolas Bonichon, Cyril Gavoille, Nicolas Hanusse, and David Ilcinkas. Connections between theta-graphs, Delaunay triangulations, and orthogonal surfaces. In *International Workshop on Graph-Theoretic Concepts in Computer Science*, pages 266–278. Springer, 2010.
- [9] Nicolas Bonichon, Cyril Gavoille, Nicolas Hanusse, and Ljubomir Perković. Plane spanners of maximum degree six. In *International Colloquium on Automata, Languages, and Programming*, pages 19–30. Springer, 2010.
- [10] Nicolas Bonichon, Cyril Gavoille, Nicolas Hanusse, and Ljubomir Perković. The stretch factor of L_1 - and L_∞ -Delaunay triangulations. In *European Symposium on Algorithms*, pages 205–216. Springer, 2012.
- [11] Nicolas Bonichon, Iyad Kanj, Ljubomir Perković, and Ge Xia. There are plane spanners of degree 4 and moderate stretch factor. *Discrete & Computational Geometry*, 53(3):514–546, 2015.
- [12] Prosenjit Bose, Paz Carmi, and Lilach Chaitman-Yerushalmi. On bounded degree plane strong geometric spanners. *Journal of Discrete Algorithms*, 15:16–31, 2012.
- [13] Prosenjit Bose, Joachim Gudmundsson, and Michiel Smid. Constructing plane spanners of bounded degree and low weight. *Algorithmica*, 42(3-4):249–264, 2005.
- [14] Prosenjit Bose, Darryl Hill, and Michiel Smid. Improved spanning ratio for low degree plane spanners. *Algorithmica*, 80(3):935–976, 2018.
- [15] Prosenjit Bose and Michiel Smid. On plane geometric spanners: A survey and open problems. *Computational Geometry*, 46(7):818–830, 2013.
- [16] Prosenjit Bose, Michiel Smid, and Daming Xu. Delaunay and diamond triangulations contain spanners of bounded degree. *International Journal of Computational Geometry & Applications*, 19(02):119–140, 2009.
- [17] Norbert Bus, Nabil H Mustafa, and Saurabh Ray. Practical and efficient algorithms for the geometric hitting set problem. *Discrete Applied Mathematics*, 240:25–32, 2018.

- [18] Paul B Callahan and S Rao Kosaraju. A decomposition of multidimensional point sets with applications to k-nearest-neighbors and n-body potential fields. *Journal of the ACM (JACM)*, 42(1):67–90, 1995.
- [19] Nicolas Catusse, Victor Chepoi, and Yann Vaxès. Planar hop spanners for unit disk graphs. In *International Symposium on Algorithms and Experiments for Sensor Systems, Wireless Networks and Distributed Robotics*, pages 16–30. Springer, 2010.
- [20] Siu-Wing Cheng, Christian Knauer, Stefan Langerman, and Michiel Smid. Approximating the average stretch factor of geometric graphs. *Journal of Computational Geometry*, 3(1):132–153, 2012.
- [21] L Paul Chew. There is a planar graph almost as good as the complete graph. In *Proceedings of the Second Annual Symposium on Computational Geometry*, 1986.
- [22] L Paul Chew. There are planar graphs almost as good as the complete graph. *Journal of Computer and System Sciences*, 39(2):205–219, 1989.
- [23] Gautam Das and Paul J Heffernan. Constructing degree-3 spanners with other sparseness properties. *International Journal of Foundations of Computer Science*, 7(02):121–135, 1996.
- [24] Adrian Dumitrescu and Anirban Ghosh. Lattice spanners of low degree. *Discrete Mathematics, Algorithms and Applications*, 8(03):1650051, 2016.
- [25] Adrian Dumitrescu and Anirban Ghosh. Lower bounds on the dilation of plane spanners. *International Journal of Computational Geometry & Applications*, 26(02):89–110, 2016.
- [26] Adrian Dumitrescu, Anirban Ghosh, and Csaba D Tóth. Sparse hop spanners for unit disk graphs. In *31st International Symposium on Algorithms and Computation (ISAAC 2020)*. Schloss Dagstuhl-Leibniz-Zentrum für Informatik, 2020.
- [27] Mohammad Farshi and Joachim Gudmundsson. Experimental study of geometric t -spanners. *Journal of Experimental Algorithmics (JEA)*, 14:3, 2009.
- [28] Greg N Federickson. Fast algorithms for shortest paths in planar graphs, with applications. *SIAM Journal on Computing*, 16(6):1004–1022, 1987.
- [29] Rachel Friederich, Matthew Graham, Anirban Ghosh, Brian Hicks, and Ronald Shevchenko. Experiments with unit disk cover algorithms for covering massive pointsets, 2022. URL: <https://arxiv.org/abs/2205.01716>.
- [30] Anirban Ghosh, Brian Hicks, and Ronald Shevchenko. Unit disk cover for massive point sets. In *International Symposium on Experimental Algorithms*, pages 142–157. Springer, 2019.
- [31] Itinerantgames. A 2d procedural galaxy with c++, Mar 2014. URL: <https://itinerantgames.tumblr.com/post/78592276402/a-2d-procedural-galaxy-with-c>.
- [32] Iyad Kanj, Ljubomir Perkovic, and Duru Türkoğlu. Degree four plane spanners: Simpler and better. *Journal of Computational Geometry*, 8(2):3–31, 2017.
- [33] Iyad A Kanj, Ljubomir Perković, and Ge Xia. On spanners and lightweight spanners of geometric graphs. *SIAM Journal on Computing*, 39(6):2132–2161, 2010.
- [34] Iyad A Kanj and Ge Xia. Improved local algorithms for spanner construction. *Theoretical Computer Science*, 453:54–64, 2012.
- [35] Rolf Klein, Martin Kutz, and Rainer Penninger. Most finite point sets in the plane have dilation > 1 . *Discrete & Computational Geometry*, 53(1):80–106, 2015.

- [36] Xiang-Yang Li and Yu Wang. Efficient construction of low weighted bounded degree planar spanner. *International Journal of Computational Geometry & Applications*, 14(01n02):69–84, 2004.
- [37] Wolfgang Mulzer. Minimum dilation triangulations for the regular n -gon. *Master's thesis, Freie Universität Berlin, Germany*, 2004.
- [38] Giri Narasimhan and Michiel Smid. Approximating the stretch factor of Euclidean graphs. *SIAM Journal on Computing*, 30(3):978–989, 2000.
- [39] Giri Narasimhan and Michiel Smid. *Geometric spanner networks*. Cambridge University Press, 2007.
- [40] Giri Narasimhan and Martin Zachariasen. Geometric minimum spanning trees via well-separated pair decompositions. *Journal of Experimental Algorithmics (JEA)*, 6:6–es, 2001.
- [41] The CGAL Project. *CGAL User and Reference Manual*. CGAL Editorial Board, 5.3 edition, 2021. URL: <https://doc.cgal.org/5.3/Manual/packages.html>.
- [42] Csaba D Toth, Joseph O'Rourke, and Jacob E Goodman. *Handbook of Discrete and Computational Geometry*. Chapman and Hall/CRC, 2017.
- [43] Christian Wulff-Nilsen. Computing the maximum detour of a plane geometric graph in subquadratic time. *Journal of Computational Geometry*, 1(1):101–122, 2010.
- [44] Ge Xia. The stretch factor of the Delaunay triangulation is less than 1.998. *SIAM Journal on Computing*, 42(4):1620–1659, 2013.

6 Appendix

6.1 Sample outputs

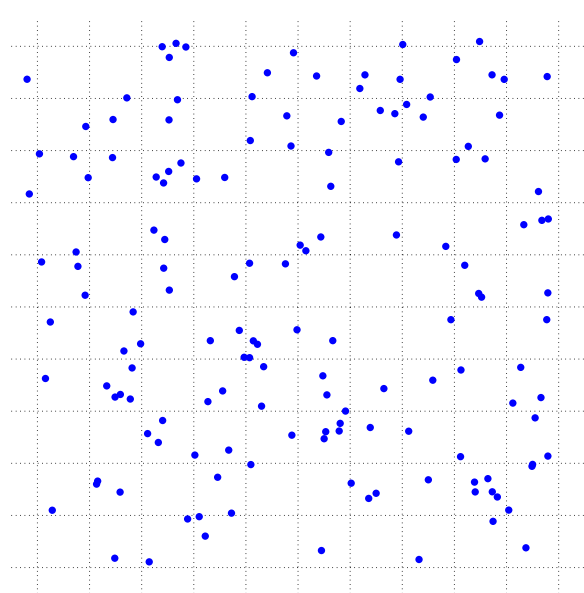


Figure 14: A 150-element pointset, drawn randomly from a square.

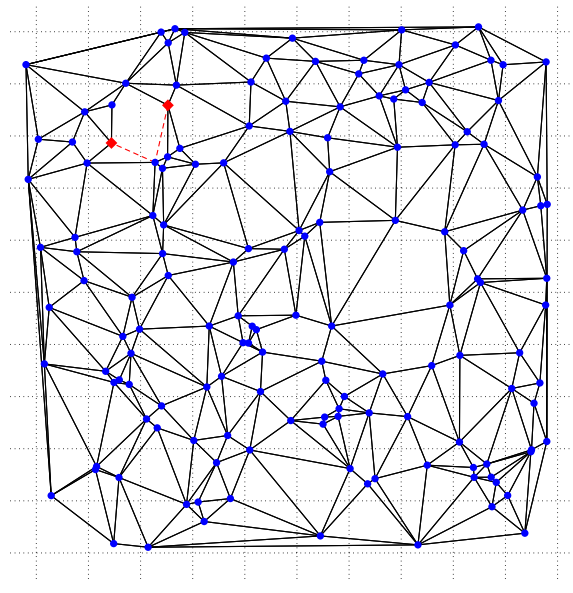


Figure 15: The spanner generated by BGS05 on the pointset shown in Fig. 14; degree: 8, stretch factor: 1.565763

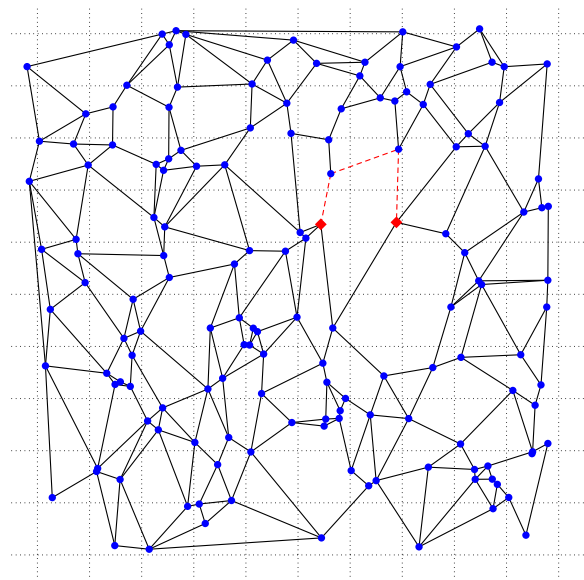


Figure 16: The spanner generated by LW04 on the pointset shown in Fig. 14; degree: 6, stretch factor: 2.602559

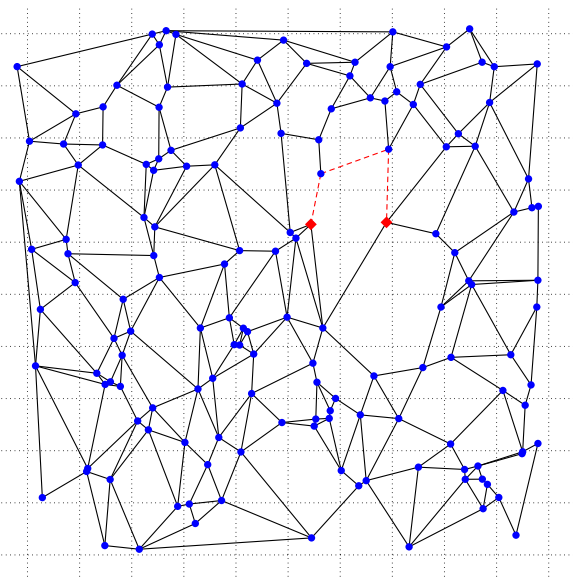


Figure 17: The spanner generated by BSX09 on the pointset shown in Fig. 14; degree: 6, stretch factor: 2.602559

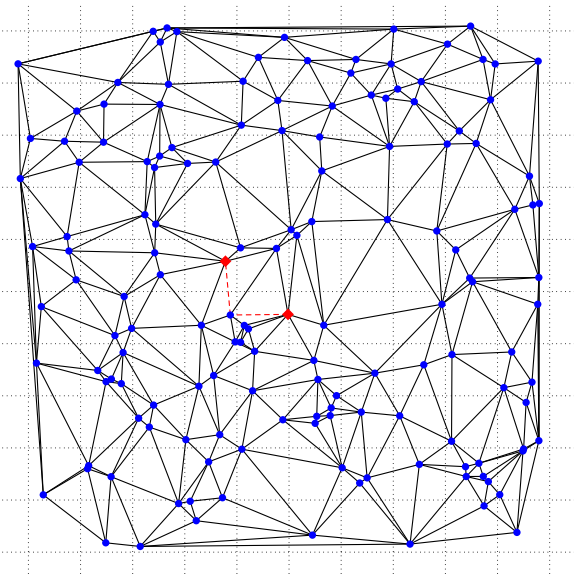


Figure 18: The spanner generated by KPX10 on the pointset shown in Fig. 14; degree: 9, stretch factor: 1.360771

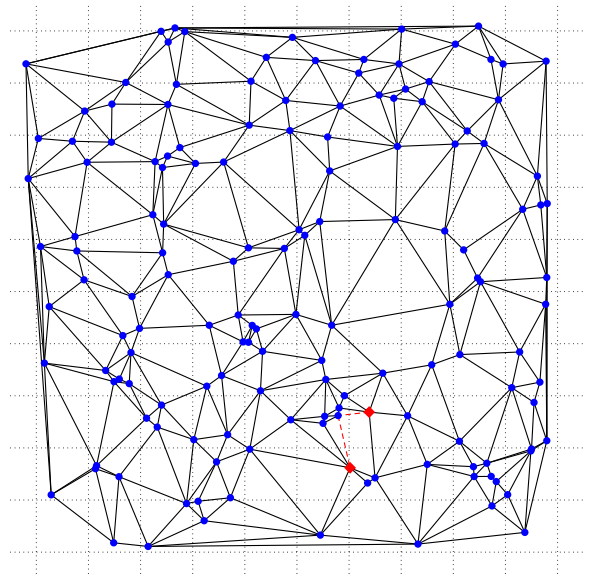


Figure 19: The spanner generated by KX12 on the pointset shown in Fig. 14; degree: 8, stretch factor: 1.440861

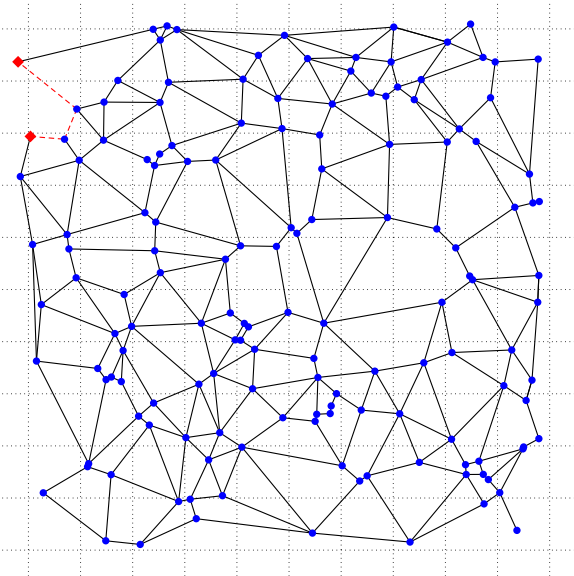


Figure 20: The spanner generated by BHS18 on the pointset shown in Fig. 14; degree: 6, stretch factor: 1.879749

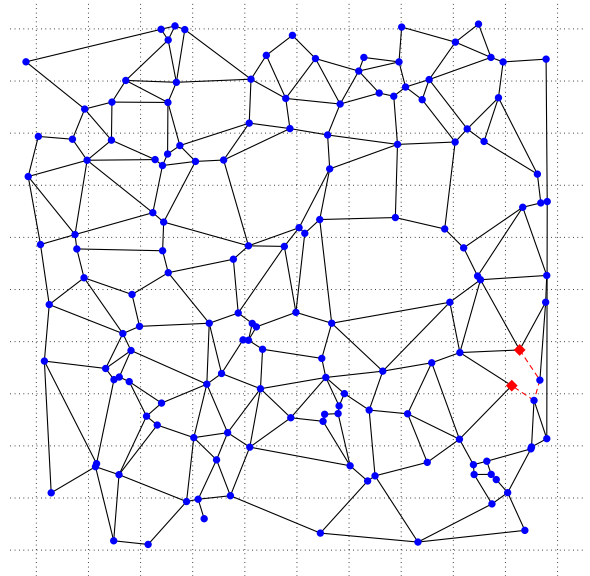


Figure 21: The spanner generated by BCC12-7 on the pointset shown in Fig. 14; degree: 6, stretch factor: 2.302473

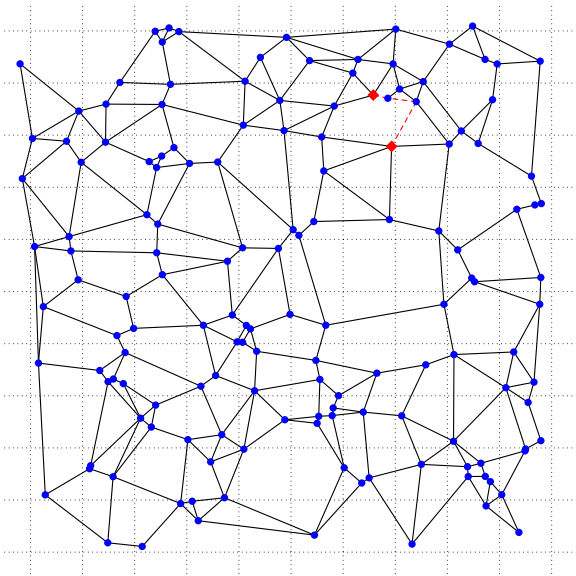


Figure 22: The spanner generated by BCC12-6 on the pointset shown in Fig. 14; degree: 6, stretch factor: 1.735716

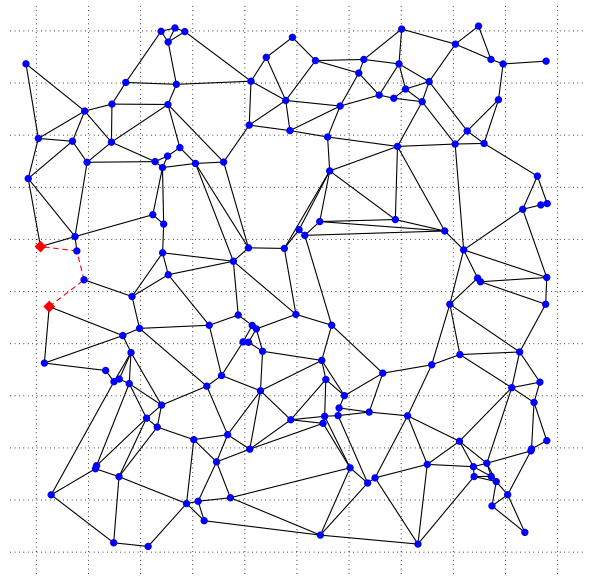


Figure 23: The spanner generated by BGHP10 on the pointset shown in Fig. 14; degree: 6, stretch factor: 1.817045

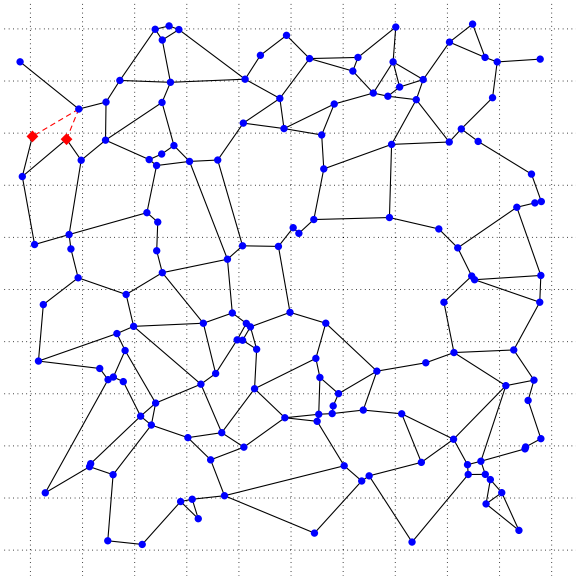


Figure 24: The spanner generated by BKPX15 on the pointset shown in Fig. 14; degree: 4, stretch factor: 2.525204

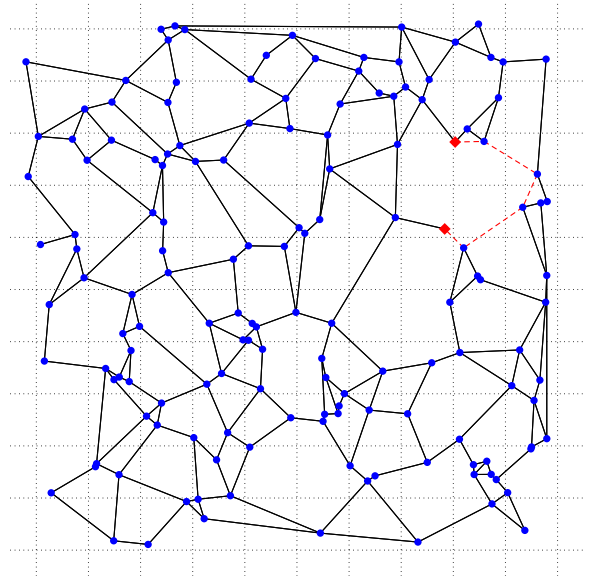


Figure 25: The spanner generated by KPT17 on the pointset shown in Fig. 14; degree: 4, stretch factor: 2.582846

6.2 A counterexample for BCC12-6

In the following, we present an 13-element pointset on which BCC12-6 fails to construct a degree-6 plane spanner. Refer to Fig. 26 for the pointset.

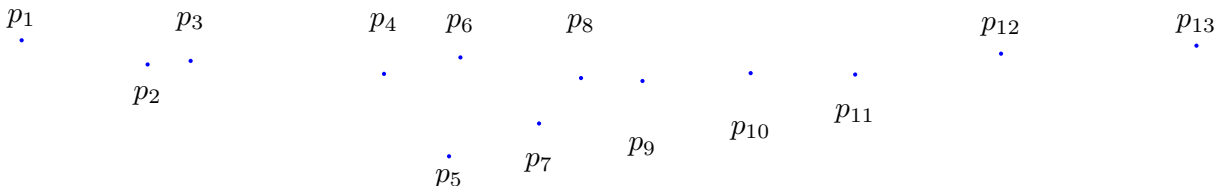


Figure 26: A set P of 13 points p_1, \dots, p_{13} . p_1 : $(-4.98845, 0.22414)$, p_2 : $(-4.23759, 0.08)$, p_3 : $(-3.98106, 0.10125)$, p_4 : $(-2.82831, 0.02396)$, p_5 : $(-2.44066, -0.46761)$, p_6 : $(-2.37275, 0.12191)$, p_7 : $(-1.90395, -0.27187)$, p_8 : $(-1.65373, -0.00109)$, p_9 : $(-1.28739, -0.01854)$, p_{10} : $(-0.642516, 0.02836)$, p_{11} : $(-0.019359, 0.02)$, p_{12} : $(0.850154, 0.14431)$, p_{13} : $(2.01517, 0.19194)$

First, BCC12-6 creates the L_2 -Delaunay triangulation of P and initializes 7 cones around every p_i , oriented such that the shortest edge incident on p_i falls on a boundary. See Figs. 27 and 28.

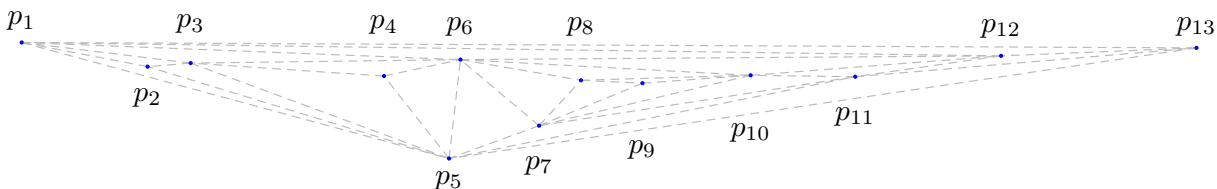


Figure 27: The L_2 -Delaunay triangulation of P .

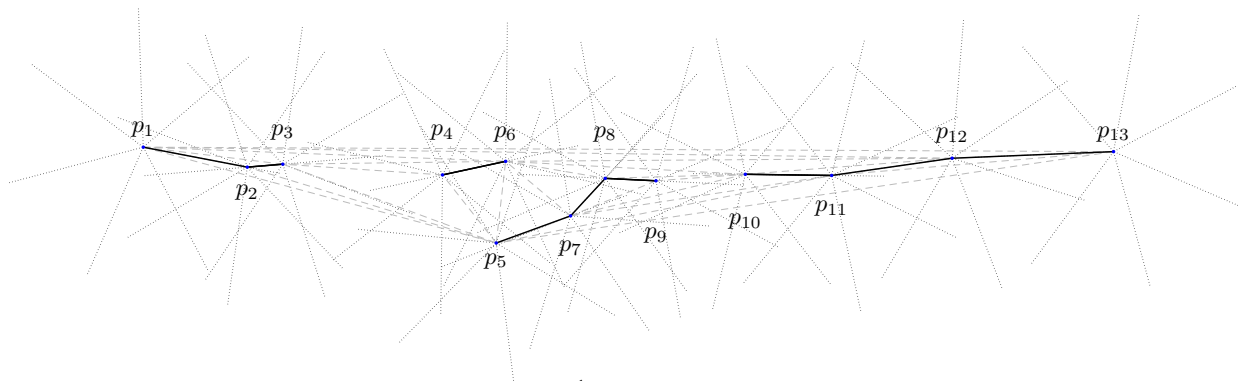


Figure 28: The cones (dotted) of each point in P with $\alpha = 2\pi/7$, oriented by the shortest edge incident on that point (bold).

Next, in Fig 29, we show the edges added by the main portion of the algorithm (excluding the edges added by Wedge_6 calls). Only $\text{Wedge}_6(p_1, p_2)$ and $\text{Wedge}_6(p_{12}, p_{11})$ calls add new edges to E^* and thus to the final spanner as well. The former call adds the two edges p_3p_6, p_6p_{12} (see Fig. 30) and the later call adds the edge p_6p_{10} (see Fig. 31). The final spanner is shown in Fig. 32. Note that p_6 has degree 7 in the spanner which violates the degree requirement of the spanners produced by BCC12-6.

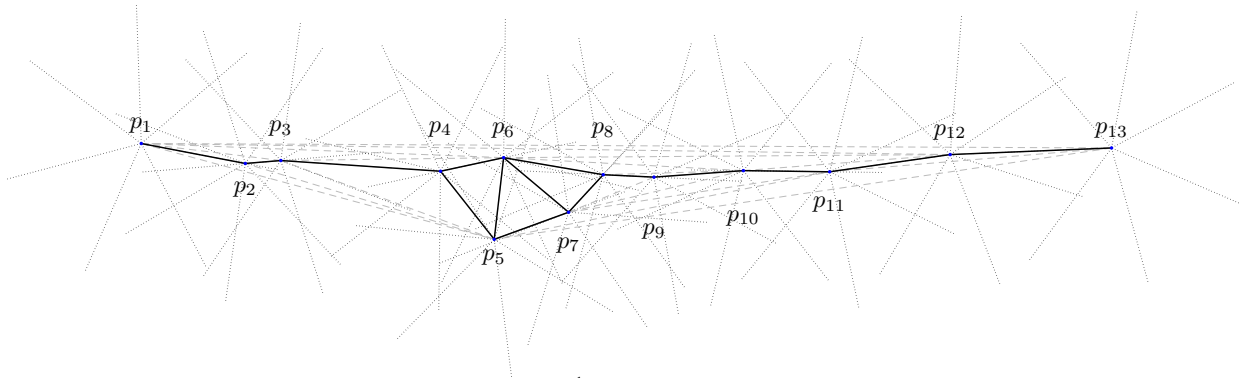


Figure 29: Edges added by the main portion of BCC12 (excluding calls to subroutine `Wedge6`).

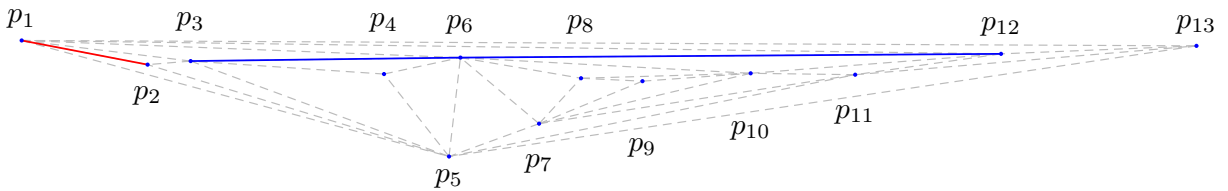


Figure 30: The edge p_1p_2 (shown in red) is added during the main portion of the algorithm and the call to `Wedge6(p1, p2)` adds the two blue edges p_3p_6 and p_6p_{12} .

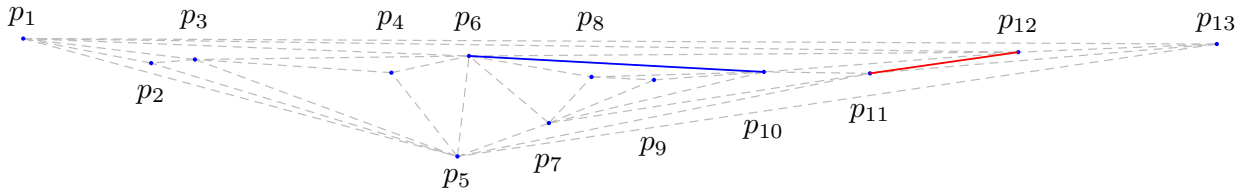


Figure 31: The edge $p_{12}p_{11}$ (shown in red) is added during the main portion of the algorithm and the call to `Wedge6(p12, p11)` adds the blue edge p_6p_{10} .

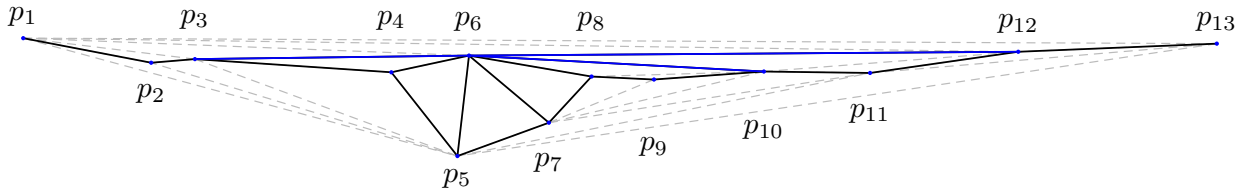


Figure 32: The resulting graph on P is a degree-7 plane spanner due to p_6 whose degree is exactly 7. Note that this graph contains the edges shown in Fig. 29 along with the blue edges shown in Fig. 30 and 31.